

DEVELOPMENT OF AN ANALYTICAL EXPRESSION FOR  
THE APPARENT EDDY VISCOSITY OF A FLUID IN  
TURBULENT MOTION IN A CIRCULAR PIPE

By

ROBERT DONAVON KERSTEN

Bachelor of Science

Oklahoma Agricultural and Mechanical College

Stillwater, Oklahoma

1949

Submitted to the Faculty of the Graduate School of  
the Oklahoma Agricultural and Mechanical College  
in partial fulfillment of the requirements  
for the degree of  
MASTER OF SCIENCE  
January, 1956

OKLAHOMA  
AGRICULTURAL & MECHANICAL COLLEGE  
LIBRARY  
JUL 16 1956

DEVELOPMENT OF AN ANALYTICAL EXPRESSION FOR  
THE APPARENT EDDY VISCOSITY OF A FLUID IN  
TURBULENT MOTION IN A CIRCULAR PIPE

Thesis Approved:

*Roger L. Flanders*  
\_\_\_\_\_  
Thesis Adviser

*Jan Peena*  
\_\_\_\_\_

*Robert Morrison*  
\_\_\_\_\_  
Dean of the Graduate School

## PREFACE

Upon completion of this the final phase of his present program of study for the degree of Master of Science in Civil Engineering, the writer wishes to gratefully acknowledge his indebtedness to the following persons who contributed greatly to the success of this undertaking.

To Dr. Clark A. Dunn, Executive Director of the Division of Engineering Research for his aid in securing the writer's appointment as Research Associate on the Pressure Surge Research Project and for his helpful encouragement during the entire program of study.

To Dr. Harold Fristoe, Project Leader, Pressure Surge Research Project and his able associates, Professors E. J. Waller and J. R. Norton whose fundamental work in more clearly defining some of the basic concepts of fluid flow pointed up the need for further basic research into the phenomena of eddy motion in turbulent flow.

To Professor Roger L. Flanders, Head, School of Civil Engineering and Professor Jan. J. Tuma, his thesis advisers for their many valuable ideas, suggestions, guidance and careful checking of all the derivations herein.

To Professor Q. B. Graves for his review of the early drafts of the manuscript and for his helpful criticisms and suggestions.

To Doctors J. H. Boggs and R. N. Maddox of O.I.T. and Dr. H. W. Smith of the Department of Mathematics for their helpful ideas, interest, encouragement and critique.

To Mr. Arlen Harris, Technician, Research and Development Laboratory, for his valuable assistance in gathering the data reported herein.

To Mrs. Fern B. Hall, Secretary, School of Civil Engineering, for her excellent work in the typing, arranging and checking of this difficult manuscript with its many equations and tables.

To the staff of the OAMC Library for their prompt, courteous and efficient assistance.

To his beloved wife, Mrs. Sue Kersten, for her constant encouragement, understanding patience and prayers without which this entire undertaking would have suffered.

January 1956  
Stillwater, Oklahoma

  
Robert D. Kersten

TABLE OF CONTENTS

<u>Chapter</u>	<u>Page</u>
I. INTRODUCTION . . . . .	1
II. PREVIOUS INVESTIGATIONS . . . . .	3
III. BASIC CONCEPTS . . . . .	5
IV. DEVELOPMENT OF AN ANALYTICAL EXPRESSION FOR THE APPARENT EDDY VISCOSITY . . . . .	13
A. Derivation . . . . .	13
B. Mathematical Verification . . . . .	19
V. EXPERIMENTAL DETERMINATION OF THE VALUE OF THE APPARENT EDDY VISCOSITY . . . . .	23
A. Equipment . . . . .	23
B. Procedure . . . . .	25
VI. EXPERIMENTAL VERIFICATION OF THE VALUE OF THE APPARENT EDDY VISCOSITY . . . . .	39
VII. APPLICATIONS OF THE APPARENT EDDY VISCOSITY . . . . .	48
A. Attenuation Coefficient . . . . .	48
B. Heat Transfer Coefficient . . . . .	49
VIII. SUMMARY AND CONCLUSIONS . . . . .	58
BIBLIOGRAPHY . . . . .	60

## LIST OF TABLES

<u>Table</u>	<u>Page</u>
1. Basic Experimental Data . . . . .	34
2. Determination of the Apparent Eddy Viscosity . . . . .	36
3. Experimental Determination of the Attenuation Coefficient . . . . .	43
4. Determination of the Attenuation Coefficient in Terms of the Apparent Eddy Viscosity . . . . .	46

## LIST OF ILLUSTRATIONS

<u>Figure</u>	<u>Page</u>
1. Comparison of Typical Velocity Distributions in Laminar and Turbulent Flow . . . . .	5
2. Definition Sketch for Velocities . . . . .	7
3. Instantaneous Distribution of Velocity in Turbulent Flow . . . . .	8
4. Turbulent Exchange of Momentum . . . . .	9
5. Illustration of Prandtl Mixing Length . . . . .	11
6. Definition Sketch for Derivation . . . . .	13
7. Illustration of Momentum Exchange . . . . .	14
8. Photograph of Experimental Apparatus . . . . .	26
9. Photograph of Instrument Table . . . . .	26
10. Photograph of Consolidated Type Pressure Cell . . . . .	27
11. Photograph of Baldwin and Consolidated Cells Mounted in Pipeline . . . . .	27
12. Typical Instrument Calibration Curve . . . . .	28
13. Plot of Mean Pressure versus Mean Velocity . . . . .	29
14. Definition Sketch for Water Hammer . . . . .	31

LIST OF ILLUSTRATIONS (cont.)

<u>Figure</u>		<u>Page</u>
15.	Typical Water Hammer Trace . . . . .	32
16.	Plot of $\Phi$ versus the Reynolds Number . . . . .	38
17.	Plot of $\Phi$ versus $\alpha_{\text{exp}}$ . . . . .	45
18.	Plot of $\Phi$ versus Reynolds Number . . . . .	56
19.	Plot of $\Phi$ versus Heat Transfer Coefficient . . . . .	57

## NOMENCLATURE

The symbols used throughout this thesis are listed below. A brief description and the descriptive units follow each symbol. F is a force, usually pounds. L is a length, usually feet. T is time, usually seconds. B is the unit of heat, usually British thermal units.  $\Theta$  is the temperature, usually degrees Fahrenheit. M is the mass unit, usually slugs (one slug = 32.2 pounds or g pounds).

- a - The velocity of propagation of a pressure wave.  $LT^{-1}$  or ft./sec.
- A - Cross-sectional area of the conduit.  $L^2$  or sq.ft.
- B - Unit of heat, British thermal unit.
- C - Constant, dimensionless.
- $c_p$  - Specific heat at constant pressure.  $BF^{-1}\Theta^{-1}$  or B/lb./ $^{\circ}$ F.
- D - Internal diameter of pipe. L or ft.
- f - Darcy-Weisbach resistance coefficient. Dimensionless.
- F - Force. F or lb.
- g - Gravitational constant.  $LT^{-2}$  or 32.2 ft./sec. $^2$ .
- h - Coefficient of heat transfer.  $BT^{-1}L^{-2}\Theta^{-1}$  or B/hr./ft. $^2$ / $^{\circ}$ F.
- k - Thermal conductivity.  $BL^{-1}\Theta^{-1}T^{-1}$  or B/ft./hr./ $^{\circ}$ F.
- $l$  - Prandtl's mixing length. L or ft.
- L - Length. L or ft.
- $\ln$  - Natural logarithm.
- n - The exponent of  $\bar{u}$  for mean flow. Dimensionless.
- $N_N$  - Nusselt number.  $\frac{hD}{k}$ . Dimensionless.
- $N_P$  - Prandtl number.  $\frac{\mu c_p}{k}$ . Dimensionless.
- $N_R$  - Reynolds number.  $\frac{D\bar{u}}{\mu}$ . Dimensionless.



- $p$  - Pressure (force per unit area)  $FL^{-2}$  or  $lb./ft.^2$  .
- $\bar{p}$  - Mean pressure drop or pressure differential in length  $L$  causing a mean flow of  $\bar{q}$  cubic feet per second.  $FL^{-2}$  or  $lb./ft.^2$  .
- $P_0$  - The initial pressure rise above the hydraulic grade line at the point of valve closure.  $FL^{-2}$  or  $lb./ft.^2$  .
- $P_x$  - The pressure rise above the hydraulic grade line at a distance  $x$  feet from the point of valve closure.  $FL^{-2}$  or  $lb./ft.^2$  .
- $\bar{q}$  - Mean volumetric flow rate.  $L^3 T^{-1}$  or  $ft.^3/sec.$
- $r$  - Variable radius of the conduit.  $L$  or  $ft.$
- $R$  - Internal radius of the conduit.  $L$  or  $ft.$
- $t$  - Time.  $T$  or  $sec.$
- $T$  - Time.  $T$ , hours or for a period of time as in integrating over a period.
- $u, v, w$  - Mean velocity at a point in the  $x, y, z$  directions respectively.  $LT^{-1}$  or  $ft./sec.$
- $\bar{u}, \bar{v}, \bar{w}$  - Mean cross-sectional velocity in the  $x, y, z$  directions respectively.  $LT^{-1}$  or  $ft./sec.$
- $u', v', w'$  - Deviation from the mean velocity at a point in the  $x, y, z$  directions respectively.  $LT^{-1}$  or  $ft./sec.$
- $u_0$  - Velocity at the centerline of the conduit in the  $x$  direction.  $LT^{-1}$  or  $ft./sec.$
- $x, y, z$  - The coordinate axes.
- $\alpha$  - The attenuation coefficient.  $L^{-1}$  or  $numeric/ft.$
- $\epsilon$  - The apparent kinematic eddy viscosity.  $L^2 T^{-1}$  or  $ft.^2/sec.$
- $\eta$  - The apparent dynamic eddy viscosity.  $FTL^{-2}$  or  $lb.sec./ft.^2$  .
- $\bar{\eta}$  - Temporal mean value of the apparent dynamic eddy viscosity.  $FTL^{-2}$  or  $lb.sec./ft.^2$  .
- $\theta$  - Temperature.  $\ominus$  , or degrees Fahrenheit.
- $\mu$  - The dynamic viscosity.  $FTL^{-2}$  or  $lb.sec./ft.^2$  .
- $\nu$  - The kinematic viscosity.  $L^2 T^{-1}$  or  $ft.^2/sec.$
- $\rho$  - The density of the fluid or mass per unit volume.  $FT^2 L^{-4}$  or  $lb.sec.^2/ft.^4$  ; or  $ML^{-3}$  or  $slugs/ft.^3$  .

- $\tau_L$  - The shearing stress in laminar flow.  $FL^{-2}$  or  $lb./ft.^2$  .  
 $\tau_e$  - The shearing stress due to the eddy motion in turbulent flow.  
 $FL^{-2}$  or  $lb./ft.^2$  .  
 $\tau$  - The total shearing stress,  $\tau_L + \tau_e$  .  $FL^{-2}$  or  $lb./ft.^2$  .  
 $\Phi$  - Ratio of the dynamic eddy viscosity to the dynamic viscosity,  
 $\frac{\bar{\eta}}{\mu}$  . Dimensionless.

#### Sign Convention

In the consideration of forces, velocities etc. in the derivations herein, up and to the right are considered positive and down and to the left are considered negative.

CHAPTER I  
INTRODUCTION

Fluid flow problems in general, are divided into two categories. These are usually designated as laminar flow and turbulent flow.

In laminar flow, the fluid moves in thin layers or lamina, one layer tending to slide with respect to its neighbor. The resulting shearing stress is caused by internal friction, i.e. the interaction between adjacent layers. There is no transfer of fluid masses between adjacent layers. The flow regime may be characterized as being very regular and orderly. As a result, fluid flow problems of this type may be readily analyzed.

If the flow is turbulent, however, there is in addition to the molecular friction an interaction between zones of flow due to momentum transfer or the transfer of fluid masses between adjacent zones of flow. The question, what is turbulence, involves more than a definition of the word. It involves a penetrating analysis of the phenomena of fluid motion to discover and recognize common features of many complex situations and to establish a clearly defined physical concept.<sup>5</sup>

For example, regular systems of eddies trail from a plucked string and are capable of description as periodic flows. The variation of velocity components with time is not, therefore, a sole criterion. The essential feature of turbulent flow which distinguishes it from the other types of flow is the presence of a random element. It has no definite periods and the flow cannot be described by a regular system of vortices however complex. Obviously, therefore the description of

turbulent flow phenomena in clear mathematical terms has been exceedingly difficult.

This thesis is intended to be a contribution to the basic principles governing turbulent flow. Particularly, an analytical expression is derived for the apparent viscosity due to the eddy motion. Use of the resulting expression is demonstrated in applications to:

1. The attenuation of a pressure wave in a liquid filled conduit.
2. The transfer of heat from a pipe wall to the fluid flowing therein.

## CHAPTER II

### PREVIOUS INVESTIGATIONS

The concept of the apparent eddy viscosity was due to Boussinesq.<sup>15a</sup> In 1877, he proposed the addition of a "molar viscosity" term to the dynamic viscosity term in the Navier-Stokes equations. No attempt was made to describe this concept of "molar viscosity" (present day eddy viscosity) in mathematical terms.

Prandtl's original work on the mixing length theory was published in Germany in 1925. Various authors have made use of this theory, until today, nearly all complete works on fluid mechanics discuss it. Prandtl's work appeared in English in 1949.<sup>12b</sup> This was the first attempt made to define mathematically the turbulent flow mixing or eddy process.

Murphree<sup>10</sup> used the results of Prandtl's mixing length theory to establish expressions for the apparent eddy viscosity. It was presumed by Murphree that there existed a turbulent boundary layer or "film" and that the apparent eddy viscosity varied as the third power from the pipe wall, while remaining essentially constant in the main body of the fluid. The resulting derivation had a pair of simultaneous equations involving three unknowns; the apparent eddy viscosity, the Fanning friction factor and the ratio of the pipe diameter to the diameter of the "film". The computation of values of the apparent eddy viscosity by this method is by a trial and error procedure, made exceedingly laborious by the fact that the equations are not independent.

The preponderance of data available<sup>13</sup> in the literature are in the form of dimensionless ratios involving velocity and temperature distri-

butions and the various fluid properties. These results offer nothing conclusive about the magnitude of the apparent eddy viscosity and only indicate what the relative magnitude would be under given conditions.

Binder<sup>4</sup> used the data obtained by Murphree in a modified version of the Kirchhoff-Helmholtz equations for the attenuation of a pressure wave traveling in a closed conduit with fair results. Waller, Fristoe and Norton<sup>18</sup> clearly demonstrated that values of the attenuation coefficient obtained by Binder's method were in error by as much as twenty percent for large amplitude vibrations in a water filled tube.

CHAPTER III  
BASIC CONCEPTS

In laminar flow the fluid moves in thin layers or lamina, one layer tending to slide with respect to its neighbor. The shearing stress  $\tau_L$  is usually written

$$\tau_L = \mu \frac{du}{dy} \quad (1)$$

where  $\frac{du}{dy}$  is the velocity gradient and  $\mu$  is the dynamic viscosity.

For turbulent flow the shearing stress is usually written as

$$\tau_L + \tau_e = \tau = (\mu + \eta) \frac{du}{dy} \quad (2)$$

where  $\eta$  is the "exchange coefficient", "mechanical viscosity" or "eddy viscosity" which is not a physical property of the fluid like  $\mu$ ,  $\rho$ ,  $\nu$  etc., but is a characteristic of motion and does depend upon the Reynolds number.

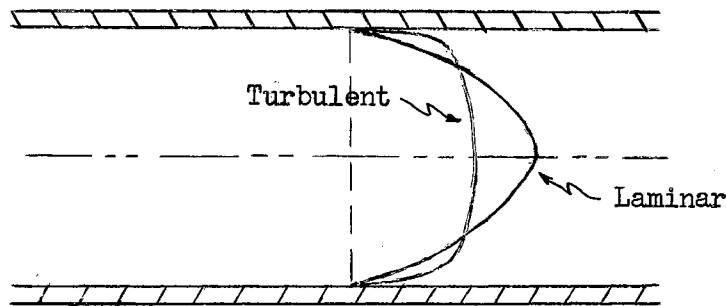


Figure No. 1

Comparison of Typical Velocity Distributions in  
Laminar and Turbulent Flow.

Turbulence originates in the boundary layer at the higher flow rates as almost sinusoidal oscillations form near the confining surface. These oscillations have been fully described by the linear theory of small oscillations of laminar boundary layers by Tollmien and Schlichting.<sup>5a</sup> It is believed that the growing waves lead to intermittent separation at the walls and the creation of minute discontinuities which are unstable. The waves tend to roll up into small scale eddies which break away from the boundary upon being disturbed.

Hence it may be seen that the randomness factor enters in through the boundary conditions. The viscosity plays a major role in the damping of the oscillations and apparently produces a phase shift between the variations of the two components of velocity. The net result being, that some fluctuations are damped out while others tend to be magnified. It must be concluded that viscosity indirectly influences the transition to turbulence.

Many mathematical models have been proposed by various authors to give a general physical picture of the turbulent flow process. In most current theory, turbulent flow is visualized as a steady motion on which is superimposed the secondary fluctuations. Prandtl's<sup>12</sup> concept of the mixing length is the theory of turbulence most familiar to engineers. These two concepts will form the basis of the mathematical derivation herein.

$$\text{Analogous to } \frac{\mu}{\rho} = \nu \quad (\text{kinematic viscosity}) \quad (3)$$

$$\text{is } \frac{\eta}{\rho} = \epsilon \quad (\text{kinematic eddy viscosity}). \quad (4)$$

Considering the dimensions involved,  $\epsilon$  should be dependent upon a length (eddy size  $l$  or mixing length) and a velocity  $v'$  or  $u'$  (eddy velocity). Just as the mean size of the eddy in turbulent flow is



governed by the boundary geometry, the mean velocity fluctuations for given boundary conditions and a given fluid depend upon the mean velocity of flow.<sup>14</sup>

Therefore,

$$\frac{\varepsilon}{\nu} \sim \frac{\bar{u} l}{\nu} = N_R$$

but  $\varepsilon = \frac{\eta}{\rho}$  and  $\nu = \frac{\mu}{\rho}$ ,

therefore<sup>14a</sup>

$$\frac{\eta}{\mu} \sim N_R. \quad (5)$$

Since  $\mu$  is essentially constant for any given situation,  $\eta$  must be directly related<sup>3</sup> to  $N_R$ . That  $\eta$  varies continually from point to point from time to time is well recognized. However, if the correlation between  $\eta$  and  $N_R$  exists<sup>12a</sup>, then there is some temporal mean value, for example<sup>2</sup>  $\bar{\eta}$ , which is representative of a given state of flow just as a given state of flow has a particular mean velocity and  $N_R$ .

Let  $u, v, w$  and  $u', v', w'$  be the mean and deviation from the mean velocities in the  $x, y, z$  directions as shown in Figure No. 2.

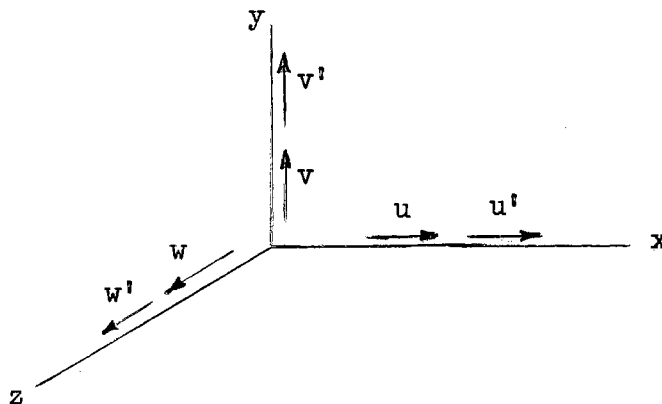


Figure No. 2

Definition Sketch for Velocities

The momentary velocity components fluctuate in a haphazard fashion, but the average velocity over a long period of time maintains a constant value. That is,

$$v = w = 0 \quad , \quad (6)$$

$$\frac{1}{T} \int_0^T u' dt = \frac{1}{T} \int_0^T v' dt = \frac{1}{T} \int_0^T w' dt = 0 \quad , \quad (7)$$

and

$$\frac{1}{T} \int_0^T u dt = \bar{u} \quad . \quad (8)$$

That these relations are true is evident from considerations of continuity.

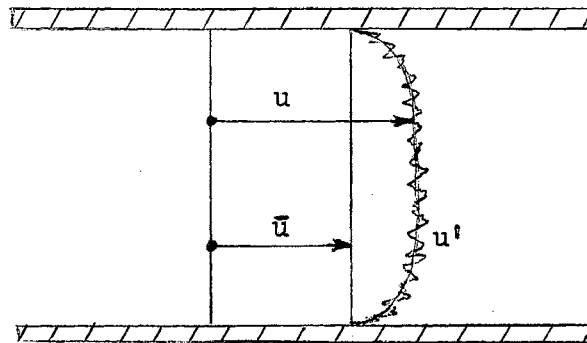


Figure No. 3

Instantaneous Distribution of Velocity  
In Turbulent Flow

While  $u'$ ,  $v'$  and  $w'$  are zero over a period of time the same is not true of the squares or products of these values. If the fluctuations were completely independent, then such values as  $u'v'$ ,  $u'w'$  and  $w'v'$  would be zero. However, quantities such as  $(u')^2$ ,  $(v')^2$  etc. would not

be zero and there would be a gradual increase in the mean velocities  $\bar{u}$ ,  $\bar{v}$  and  $\bar{w}$  due to the eddy motion. Any change in  $\bar{v}$  and  $\bar{w}$  from a zero value would violate the conditions of continuity. An increase in  $\bar{u}$  from any previously established value would violate the hypothesis of a steady flow condition. Thus, there must be some relation between the quantities  $u'v'$  and  $(u')^2$  etc. which permits the above outlined hypotheses to be fulfilled, or in other words, the existence of a correlation between  $u'$ ,  $v'$  and  $w'$  must be admitted. That is, the turbulent friction or apparent shearing stress is different from zero only when there is a correlation between  $u'$ ,  $v'$  and  $w'$ .<sup>12c</sup>

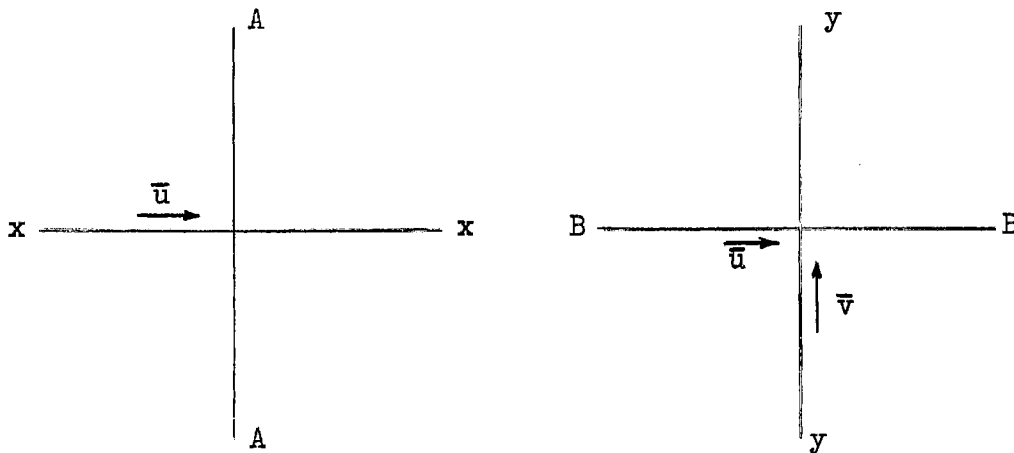


Figure No. 4

#### Turbulent Exchange of Momentum

The mass crossing plane AA in time  $dt$  is  $\rho \bar{u} dt$  and the x component of velocity is  $\bar{u}$ ; the momentum transfer in time  $dt$  is  $\rho \bar{u}^2 dt$  or over a long period  $T$  is

$$\frac{1}{T} \int_0^T \rho \bar{u}^2 dt = \rho \bar{u}^2, \quad (9)$$

but

$$\bar{u}^2 = (u + u')^2 = u^2 + 2uu' + \overline{(u')^2}.$$

By definition, (see Eq. 7)  $u'$  over a period of time is zero. Therefore, the quantity  $2uu' = 0$ . Whence,

$$\rho \bar{u}^2 = \rho u^2 + \rho \overline{(u')^2}. \quad (10)$$

Therefore, there is added to the momentum of the steady motion the momentum due to the temporal mean value of the square of the velocity fluctuations<sup>12d.</sup>

The mass crossing plane BB in time  $dt$  is  $\rho \bar{v} dt$  and the x component of velocity is  $\bar{u}$ . Hence, the momentum transfer is  $\rho \bar{u} \bar{v} dt$  in time  $dt$ , or

$$\frac{1}{T} \int_0^T \rho \bar{u} \bar{v} dt = \rho \bar{u} \bar{v} \quad (11)$$

in time  $T$ . But  $\bar{u} \bar{v} = (u + u')(v + v') = uv + \overline{uv'} + \overline{u'v} + \overline{u'v'}$  where again the second and third terms on the right are zero due to  $v'$  and  $u'$  being zero over the period by definition. Therefore,

$$\rho \bar{u} \bar{v} = \rho uv + \rho \overline{u'v'}. \quad (12)$$

Thus, also a term due to the variations in velocities has to be added to that of the steady motion. The reaction corresponding to  $\rho \overline{u'v'}$  which is exerted on unit area is a force in the direction of the x axis acting on an area perpendicular to the y axis, i.e., a shearing stress. Therefore, the apparent shearing stress due to the eddy motion is

$$\tau_e = - \rho \overline{u'v'}. \quad (13)$$

The negative sign is necessary to give a positive shearing stress since  $\overline{(u'v')}$  is always a negative quantity, i.e., a positive  $u'$  is associated with a negative  $v'$  and vice versa<sup>15</sup>. In order to obtain a

formula for practical use it is necessary to express  $u'$  and  $v'$  in terms of quantities related to the mean velocity.

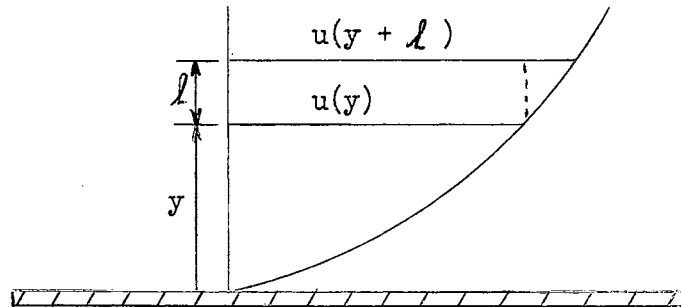


Figure No. 5

Illustration of Mixing Length

Some length,  $l$  may be envisioned<sup>12e</sup> through which the particles of fluid move relative to the rest of the fluid before they lose their identity by mixing with the surrounding fluid. If a particle is displaced from a position  $y$  (see Figure No. 5) with a velocity  $u(y)$  through a distance  $l$  to a point where the velocity is  $u(y+l)$ , the difference in velocity is,

$$u(y+l) - u(y) \doteq l \frac{du}{dy} \doteq u' \quad , \quad (14)$$

similarly

$$v' \doteq l \frac{du}{dy} \quad , \quad (15)$$

whence

$$\tau_e = \rho l^2 \left| \frac{du}{dy} \right| \frac{du}{dy} \quad (16)$$

or

$$\tau_e = -\rho \overline{v'l} \frac{du}{dy} \quad . \quad (17)$$

Let 
$$\eta = -\rho \overline{v'l} \quad (18)$$

then 
$$\tau_e = \eta \frac{du}{dy} \quad (19)$$

or as is usually written for turbulent flow, the total shearing stress becomes

$$\tau = (\mu + \eta) \frac{du}{dy} . \quad (2)$$

The results of the Prandtl mixing length theory as expressed in Eq. 18 will be used in the following derivation.

CHAPTER IV  
 DEVELOPMENT OF AN ANALYTICAL EXPRESSION FOR  
 THE APPARENT EDDY VISCOSITY

A. DERIVATION

In uniform motion with no acceleration, the summation of the pressure forces, forces due to momentum transfer and the tangential friction forces must be zero. On choosing a point at which to describe the fluid flow regime it is found that all the velocity components are in perpetual and continual fluctuation. (See Figure No. 2 and Eq.'s 6, 7 and 8).

However, from the conditions expressed in Eq.'s 6, 7 and 8 the average velocity over a sufficiently long period of time maintains a constant value. This being true, the net momentum transfer over the same period of time is zero and the summation of forces is possible. The two-dimensional flow of a fluid under turbulent conditions is pictured in Figure No. 6.

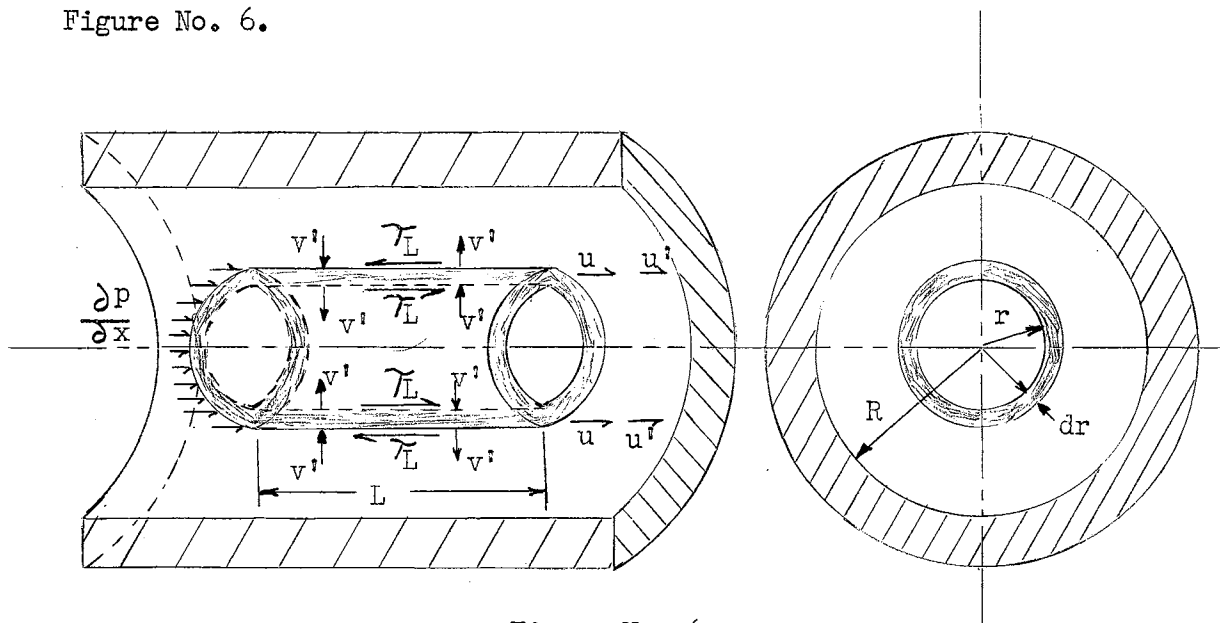


Figure No. 6

Definition Sketch for Derivation

The relative radial velocity perpendicular to the mean velocity  $u$  is  $v'$ ; length of shell is  $L$  and is of such length that the average value of  $v'$  over the inside and outside of the shell is zero.

Summation of Forces on the Inside of the Shell

The momentum transfer into the shell due to  $u'$  and  $v'$  per unit length is  $2\pi r \rho \overline{v'u'}$ . The average gain of momentum to the shell is  $2\pi rL \rho \overline{v'u'}$  which acts as a force directed to the right.



Positive Momentum Exchange

Negative Momentum Exchange

Figure No. 7

The viscous force on the inside of the shell is directed toward the right and is

$$2\pi r \mu L \left( \frac{\partial u}{\partial r} \right).$$

The total force on the inside of the shell is then

$$2\pi rL \left( -\mu \frac{\partial u}{\partial r} + \rho \overline{v'u'} \right).$$

The minus sign is necessary because the velocity gradient is negative and



the force acts to the right.

### Summation of Forces on the Outside of the Shell

The force exerted to the left by the momentum transfer from the outside of the shell is

$$-(2 \pi r L \rho \overline{v'u'}) + \frac{\partial}{\partial r} [2 \pi r L \rho \overline{v'u'}] dr$$

and the viscous force directed to the left is

$$-(-2 \pi r L \mu \frac{\partial u}{\partial r} - \frac{\partial}{\partial r} [2 \pi r L \mu \frac{\partial u}{\partial r}] dr)$$

where the minus sign is again needed to indicate the proper sense.

Therefore the total force on the outside of the shell is

$$-2 \pi L \left\{ -r \mu \frac{\partial u}{\partial r} + r \rho \overline{v'u'} + \frac{\partial}{\partial r} [r(-\mu \frac{\partial u}{\partial r} + \rho \overline{v'u'})] dr \right\}.$$

### Effect of the Pressure Gradient

The force exerted by the pressure gradient is

$$\frac{\partial p}{\partial x} (2 \pi r L) dr$$

### Summation of All Forces

Adding these forces and setting the sum equal to zero:

$$2 \pi r L (-\mu \frac{\partial u}{\partial r} + \rho \overline{v'u'}) - 2 \pi L \left\{ -r \mu \frac{\partial u}{\partial r} + r \rho \overline{v'u'} + \frac{\partial}{\partial r} [r(-\mu \frac{\partial u}{\partial r} + \rho \overline{v'u'})] dr \right\} + \frac{\partial p}{\partial x} (2 \pi r L) dr = 0$$

simplifying,

$$\frac{d}{dr} \left[ r \left( \mu \frac{\partial u}{\partial r} - \rho \overline{v'u'} \right) \right] dr = \frac{\partial p}{\partial x} r . \quad (20)$$

The term  $\rho \overline{u'v'}$  in Eq. 20 represents the transfer of momentum per unit area across the shell boundary. Physically, this transfer is due to groups of molecules being thrown by the component of the eddy currents perpendicular to the mean velocity from one zone of flow to another. The first zone may correspond to a higher or lower value of the mean velocity ( $u$ ) than the second. If higher, the value of  $u'$  is positive and, if lower,  $u'$  is negative. (See Figure No. 7).

Since  $u'$  may be regarded as equal to  $\frac{\partial u}{\partial r} l$  where  $l$  is the distance between zones of flow, (or Prandtl's mixing length) then  $-\rho \overline{u'v'}$  in Eq. 20 may be replaced by

$$-\rho \overline{v'l} \frac{\partial u}{\partial r} .$$

But  $-\rho \overline{v'l}$  is mass times velocity times length of  $\rho \epsilon$  which is  $\eta$ . (See Eq. 4).

Let

$$\eta = -\rho \overline{v'l} , \quad (18)$$

then

$$-\rho \overline{v'u'} = \eta \frac{\partial u}{\partial r} \quad (21)$$

and Eq. 20 becomes

$$\frac{d}{dr} \left[ r \left( \mu + \eta \right) \frac{\partial u}{\partial r} \right] = \frac{\partial p}{\partial x} r .$$

$$\text{Let } \frac{\partial p}{\partial x} = -\frac{\bar{p}}{L}$$

then

$$\frac{\partial}{\partial r} \left[ r(\mu + \eta) \frac{\partial u}{\partial r} \right] = -\frac{\bar{p}r}{L} \quad (22)$$

### Integration of Differential Equation

Eq. 22 can be integrated if  $\eta$  may be assumed constant<sup>7</sup> for a given flow regime, for example, a temporal mean value  $\bar{\eta}$ .

Then Eq. 22 becomes

$$\frac{\partial}{\partial r} \left[ r(\mu + \bar{\eta}) \frac{\partial u}{\partial r} \right] = -\frac{\bar{p}r}{L}$$

Performing the integration,

$$r(\mu + \bar{\eta}) \frac{\partial u}{\partial r} = -\frac{\bar{p}r^2}{2L} + C_1$$

Since  $\frac{\partial u}{\partial r} = 0$  when  $r = 0$ ;  $C_1 = 0$

and

$$\frac{\partial u}{\partial r} = -\frac{\bar{p}r}{2L(\mu + \bar{\eta})} \quad (23)$$

Integrating Eq. 23

$$u = -\frac{\bar{p}r^2}{4L(\mu + \bar{\eta})} + C_2$$

When  $r = 0$ ;  $u = u_0$

therefore  $C_2 = u_0$

and

$$u = u_0 - \frac{\bar{p}r^2}{4L(\mu + \bar{\eta})} \quad (24)$$

From the continuity equation

$$\bar{q} = A\bar{u}$$

or

$$\bar{q} = \int_0^R 2\pi r u dr \quad . \quad (25)$$

Substituting Eq. 24 in Eq. 25 and integrating

$$\bar{q} = \pi R^2 u_0 - \frac{\pi \bar{p} R^4}{8L(\mu + \bar{\eta})} \quad .$$

Since

$$\bar{u} = \frac{\bar{q}}{A} = \frac{\bar{q}}{\pi R^2}$$

$$\bar{u} = u_0 - \frac{\bar{p} R^2}{8L(\mu + \bar{\eta})} \quad . \quad (26)$$

From the Karman-Prandtl equation for the velocity distribution in turbulent flow, it may be shown that the ratio of the maximum or center-line velocity ( $u_0$ ) to the mean velocity ( $\bar{u}$ ) is<sup>14b</sup>

$$\frac{u_0}{\bar{u}} = 1.43 \sqrt{f} + 1 \quad , \quad (27)$$

where  $f$  is the Darcy-Weisbach resistance coefficient as defined by

$$\bar{p} = f \frac{L}{D} \frac{\bar{u}^2}{2} \rho \quad . \quad (28)$$

Substituting Eq. 27 in Eq. 26

$$\bar{u} = \frac{\bar{p} R^2}{8L(\mu + \bar{\eta})(1.43 \sqrt{f})} \quad . \quad (29)$$

Rearranging,

$$\bar{\eta} = \frac{\bar{p} R^2}{8L(1.43 \sqrt{f})\bar{u}} - \mu \quad . \quad (30)$$

Eq. 30 is the defining equation for the apparent eddy viscosity. A relatively simple expression results in which all quantities are readily measurable. It should be noted here that even at relatively low Reynolds numbers, the effect of the dynamic viscosity is slight. In which case the apparent eddy viscosity becomes a function of the pressure gradient, pipe size and friction factor. The primary importance of this fact is that the apparent eddy viscosity becomes essentially temperature independent.

#### B. MATHEMATICAL VERIFICATION

Inspection of Eq. 30 shows that it is dimensionally correct.

A quick check on the mathematical soundness of the preceding derivation may be obtained by assuming the flow to be laminar. ( $\overline{\eta} = 0$ ). Equation 26 then reduces to

$$\bar{u} = u_o - \frac{\bar{p}R^2}{8L\mu} \quad (26a)$$

For laminar flow conditions the well known parabolic velocity distribution applies<sup>14c</sup>, whence,

$$\bar{u} = \frac{1}{2} u_o \quad \text{or} \quad 2\bar{u} = u_o .$$

Then Eq. 26a becomes

$$\bar{u} = \frac{\bar{p}R^2}{8L\mu}$$

or

$$\mu = \frac{\bar{p}R^2}{8L\bar{u}} = \frac{\bar{p}D^2}{32L\bar{u}} \quad (31)$$

which is the well known equation of Poiseuille<sup>14d</sup>.

To further verify the superposition principle for turbulent flow and the exactness of Prandtl's mixing length theory, Eq. 30 will be derived from the Navier-Stokes equations. Consider the Navier-Stokes equation

for the x direction<sup>8</sup> as modified by Boussinesq<sup>15a</sup>;

$$\frac{F_x}{\rho} = \frac{1}{\rho} \frac{\partial (p + \gamma h)}{\partial x} - \frac{(\mu + \bar{\eta})}{\rho} \left[ \frac{1}{3} \frac{\partial \psi}{\partial x} + \nabla^2 u \right] \quad (32)$$

where

$$\psi = \frac{\partial u}{\partial x} + \frac{\partial v}{\partial y} + \frac{\partial w}{\partial z}$$

and

$$\nabla^2 u = \frac{\partial^2 u}{\partial x^2} + \frac{\partial^2 u}{\partial y^2} + \frac{\partial^2 u}{\partial z^2} .$$

Assuming a constant elevation,  $\gamma h = \text{constant}$  and  $\frac{\partial(\gamma h)}{\partial x} = 0$ .

Therefore, Eq. 32 reduces to

$$F_x = \frac{\partial p}{\partial x} - (\mu + \bar{\eta}) \left[ \frac{1}{3} \frac{\partial \psi}{\partial x} + \nabla^2 u \right] \quad (32a)$$

Since  $F_x = ma$  according to Newton's second law,

$$\rho \frac{du}{dt} = \frac{\partial p}{\partial x} - (\mu + \bar{\eta}) \left[ \frac{1}{3} \frac{\partial \psi}{\partial x} + \nabla^2 u \right] . \quad (32b)$$

The density,  $\rho$ , was assumed to be constant, (i.e. fluid incompressible) therefore, the divergence<sup>11</sup> of the velocity vector must be zero and

$$\frac{\partial \psi}{\partial x} = 0 .$$

In addition, the velocity remains constant in the x direction due to the constant pressure gradient and uniformity of the flow section.

Whence

$$\frac{\partial^2 u}{\partial x^2} = 0 \quad \text{and} \quad \frac{du}{dt} = 0$$

and Eq. 32b becomes

$$\frac{\partial p}{\partial x} = (\mu + \eta) \left[ \frac{\partial^2 u}{\partial y^2} + \frac{\partial^2 u}{\partial z^2} \right] \quad (32c)$$

Transforming into cylindrical co-ordinates and assuming

$$\begin{aligned} \frac{\partial p}{\partial x} &= -\frac{\bar{p}}{L}, \\ -\frac{\bar{p}}{L} &= \frac{(\mu + \eta)}{r} \frac{\partial}{\partial r} \left( r \frac{\partial u}{\partial r} \right). \end{aligned} \quad (32d)$$

Integrating

$$-\frac{\bar{p}r}{2L(\mu + \eta)} = \frac{\partial u}{\partial r} + C_1.$$

At

$$r = 0; \quad \frac{\partial u}{\partial r} = 0 \quad \text{whence } C_1 = 0$$

and

$$\frac{\partial u}{\partial r} = -\frac{\bar{p}r}{2L(\mu + \eta)}. \quad (23)$$

Integrating

$$u = -\frac{\bar{p}r^2}{4L(\mu + \eta)} + C_2$$

where  $r = 0; \quad u = u_0$  and therefore  $C_2 = u_0$

and Eq. 24 results.

$$u = u_0 - \frac{\bar{p}r^2}{4L(\mu + \eta)} \quad (24)$$

Substituting into the continuity equation (Eq. 25) and integrating, Eq. 26 may be derived. Making use of Eq. 27 for the ratio of the center-line velocity to the mean velocity Eq. 30 is obtained:

$$\bar{\eta} = \frac{\bar{\rho} R^2}{8L(1.43 \sqrt{f})\bar{u}} - \mu \quad (30)$$

This is particularly interesting from the standpoint that as late as 1930 it was widely believed that the Navier-Stokes equations could not be applied to turbulent flow<sup>5b</sup> and the inclination was to discredit Boussinesq's concept of "molar" viscosity (present day eddy viscosity)<sup>15a</sup>.



CHAPTER V  
EXPERIMENTAL DETERMINATION  
OF  
THE VALUE OF THE APPARENT EDDY VISCOSITY

Examination of Eq. 30 indicates that for a pipe of given dimensions and known roughness, measurement of the mean pressure gradient and the mean velocity will permit calculation of values of the apparent eddy viscosity for a given fluid.

A. EQUIPMENT

The pilot pipeline constructed by the personnel of the Pressure Surge Research Project was used to obtain the data reported herein. This system consisted of 2,082 feet of standard wrought iron pipe one and one half inches in diameter, two storage tanks (322 gallon capacity), an air compressor system (0-125 psi capacity), the necessary valves, fittings and gages, a Midwestern recording oscillograph and five Consolidated Engineering Type 4.311 pressure cells (0-250 psi capacity).

The pipeline was looped four times around the periphery of the Engineering Building basement, terminating at the storage tanks. The individual components were joined together by Groovagrip connections and securely anchored to concrete piers approximately ten feet on centers by means of wooden clamps. Figure 8 is a picture of the storage tanks and related equipment. The piping may be seen on the piers in the background. (A) is the air compressor; (B) is the west tank with gage glass on the side and air regulator valve on top; (C) is the east tank, identical in detail to the west tank; (D) is the differential mercury manometer used to determine the general range of pressure differential between the west

and east tanks.

Figure 9 is a photograph of the instrument table showing (A) the Midwestern oscillograph, (B) the camera for the oscillograph and (C) the control panel. Figure 10a is a photograph of the Consolidated Engineering Type 4.311 pressure cell. Figure 10b shows the strain gage wire of the internal mechanism of the cell.

Figure 11 is a photograph showing a Baldwin type pressure cell (A) mounted opposite a Consolidated type pressure cell (B) in the pilot pipeline. At the extreme left of the picture is a quick opening valve.

The errors in instrumentation and in reading the oscillograph traces are the governing factors in the experimental precision. An estimate of the probable error in obtaining the experimental pressure amplitudes may be found by considering the following independent errors that may exist:

1. The pickup linearity =  $\pm .39\%$  of full-scale pressure, or  
 pickup linearity =  $\pm .39 \frac{(250)}{(100)} = \pm .975$  psi.

2. The pickup hysteresis =  $\pm .39\%$  of full scale pressure or  
 pickup hysteresis =  $\pm .975$  psi.

3. The galvanometer hysteresis =  $\pm 1\%$  of three inches deflection,  
 or the galvanometer hysteresis =  $\pm .03$  inches, which is approximately  
 $\pm 2$  psi from the calibration curves.

4. The trace reading error is estimated as being  $\pm .03$  inches  
 (thickness of line on trace) or  $\pm 2$  psi.

If these estimates represent two standard deviations of the individual error, then the standard deviation of the total error is the square root of the sum of the squares of the standard deviations of the

individual errors.

$$\sigma_{\text{error}} = \sqrt{\left(\frac{.975}{2}\right)^2 + \left(\frac{.975}{2}\right)^2 + \left(\frac{2}{2}\right)^2 + \left(\frac{2}{2}\right)^2} = 1.575 \text{ psi.}$$

This means that 95% of the experimental values should fall in a band  $\pm 3.15$  psi (i.e. two standard deviations) from their mean value. A typical instrument calibration curve is shown in Figure 12.

The relationship between the mean velocity  $\bar{u}$  and the mean pressure  $\bar{p}$  was determined by plotting the differential pressure between the end points of the line under various steady flow conditions versus the mean velocity. The mean velocity was determined by measuring the time necessary for a given volume to flow and using the continuity relationship for the steady motion,  $\bar{u} = \frac{\bar{q}}{A}$ . The equation (see Figure 13)

$$\bar{p} = 3.24 \bar{u}^{1.885} \quad (33)$$

is the resulting experimental relationship or calibration equation for this pipeline connecting differential pressure (psi) and mean velocity (fps).

#### B. PROCEDURE

The data necessary to determine the value of the apparent eddy viscosity may be obtained as outlined below. Knowing the pipe dimensions and the fluid properties:

$$L = 2082 \text{ feet}$$

$$D = 1.61 \text{ inches} = .134 \text{ feet}$$

$$\rho = 1.94 \text{ lb. sec}^2/\text{ft}^4 \text{ (at } 70^\circ \text{ F)}$$

$$\mu = 2.04 \times 10^{-5} \text{ lb. sec/ft}^2 \text{ (at } 70^\circ \text{ F)}$$

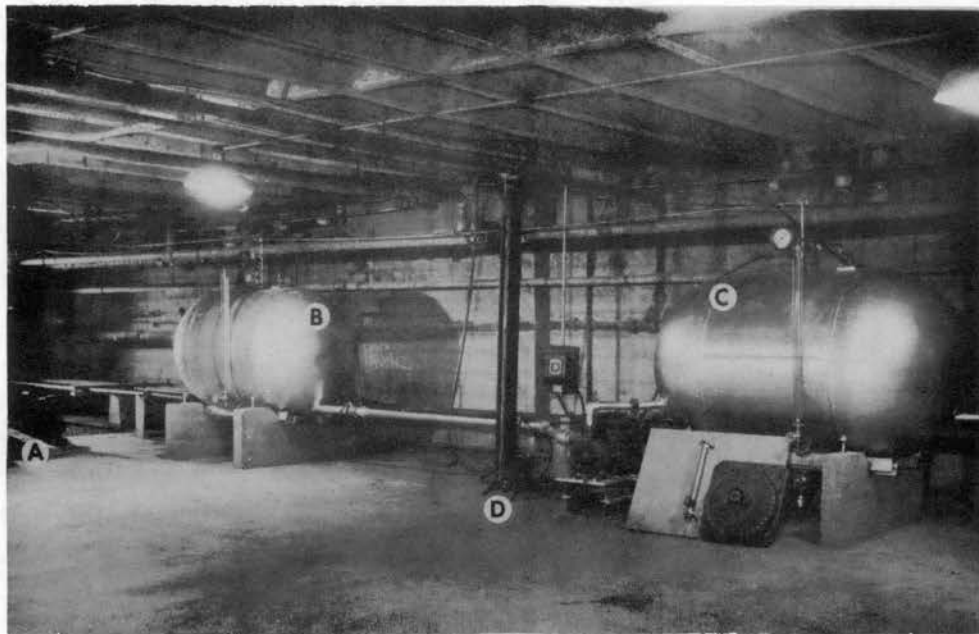


Figure No. 8  
Experimental Apparatus

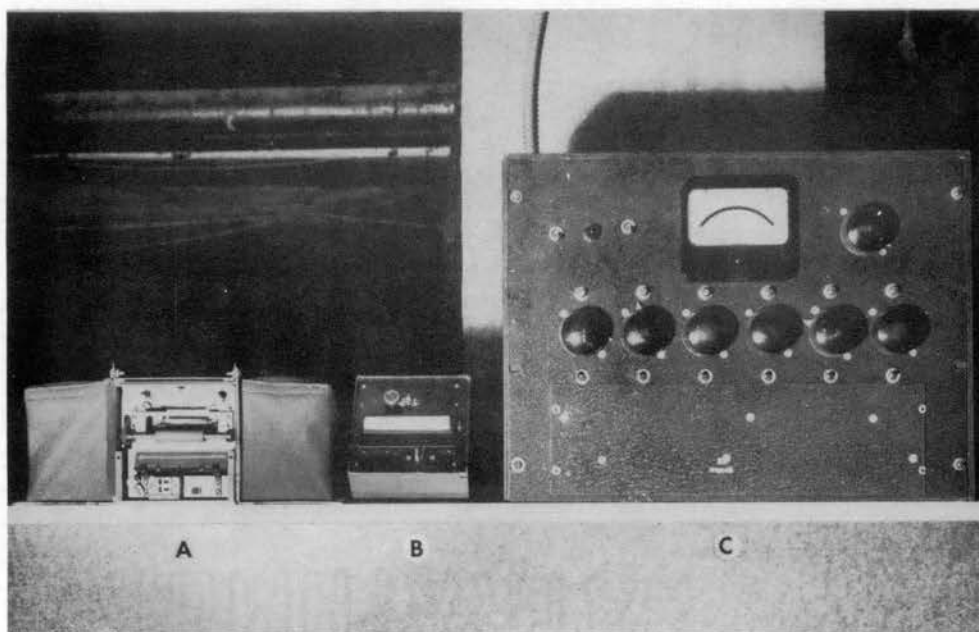


Figure No. 9  
Instrument Table

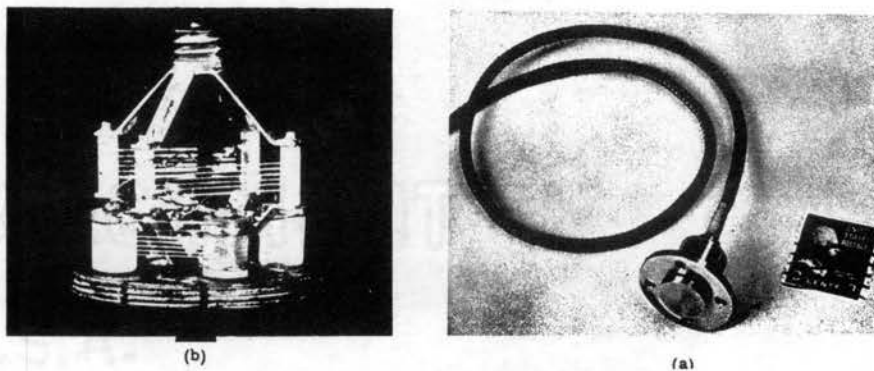


Figure no. 10  
C. E. Pressure Pickup

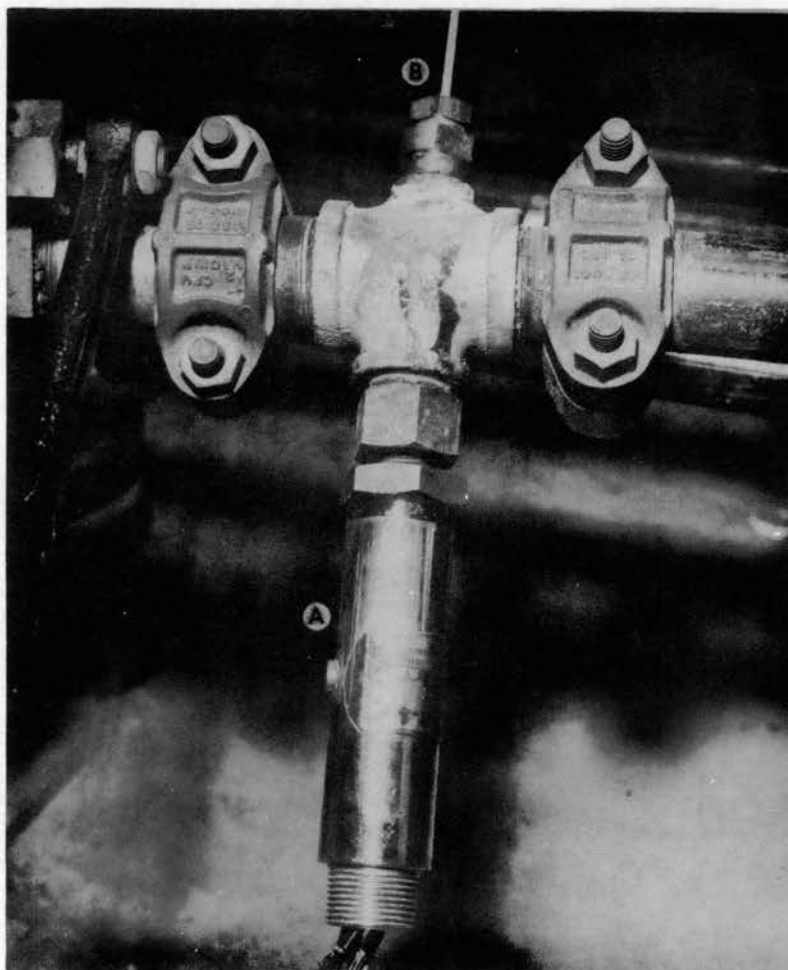
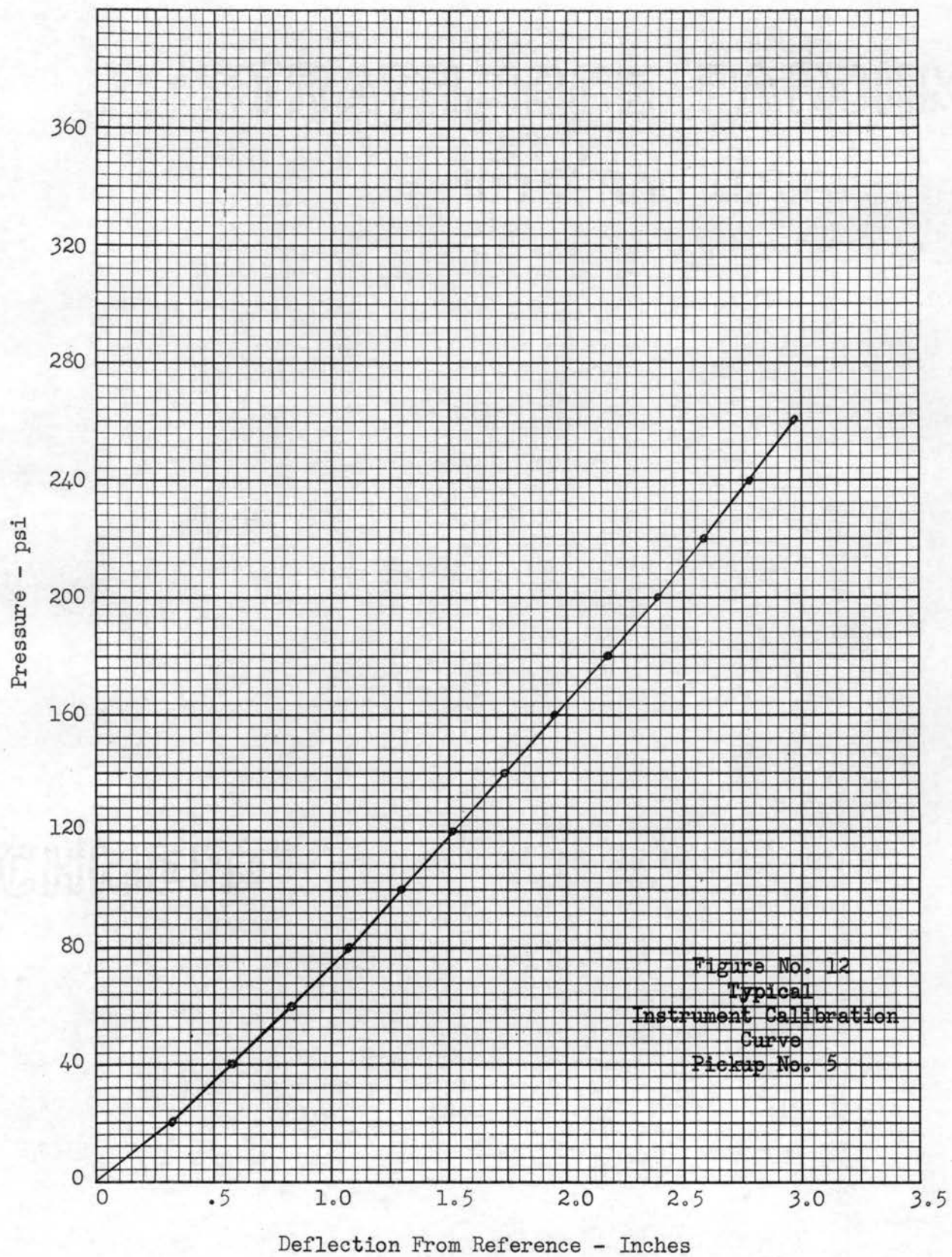


Figure No. 11  
Pickups Mounted in the Line



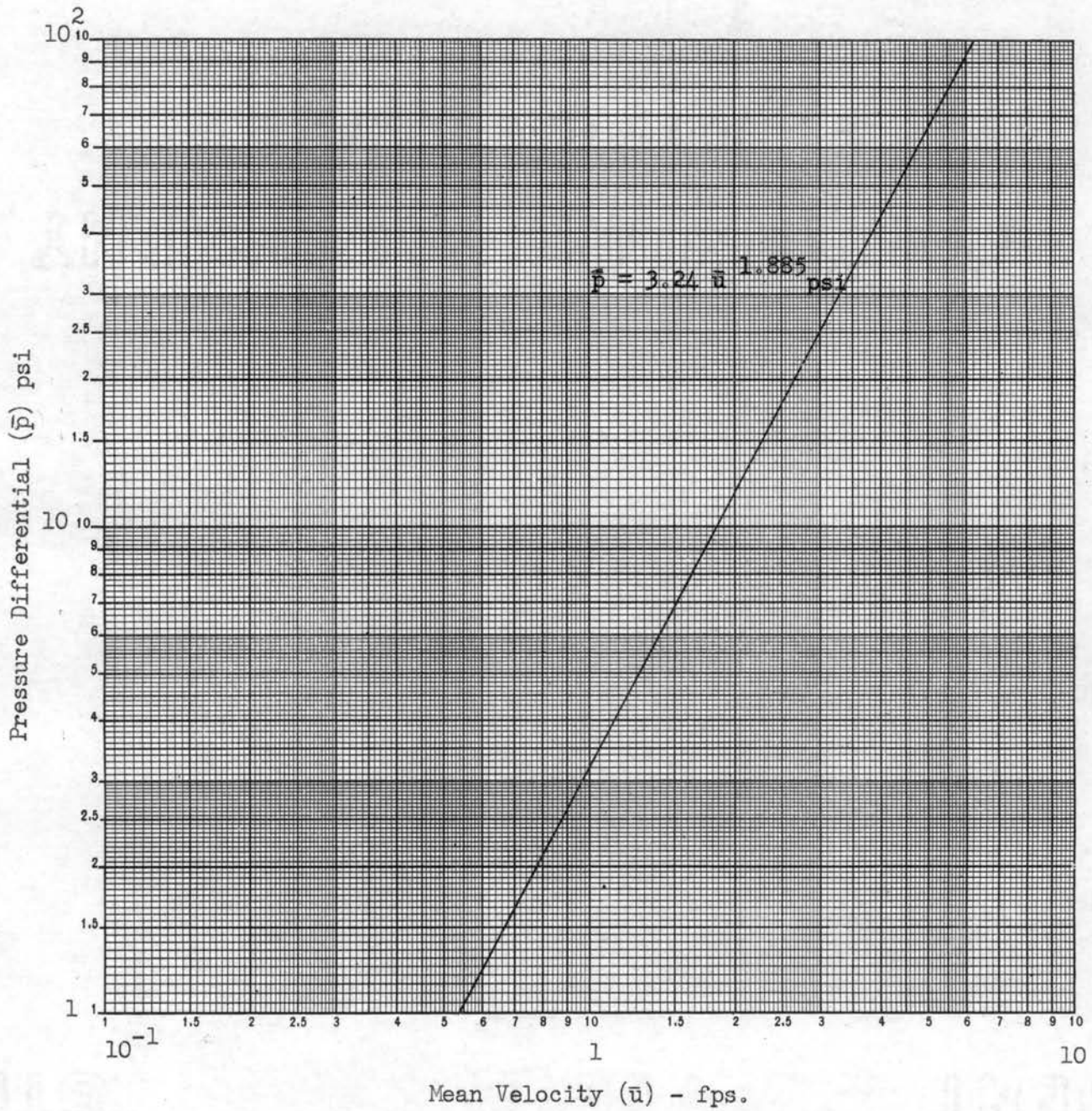


Figure No. 13

Mean Velocity vs. Pressure Differential

Eq. 30 reduces to

$$\bar{\eta} = 2.72 \times 10^{-5} \frac{\bar{p}}{\bar{u} \sqrt{f}} - \mu \quad (34)$$

It is now apparent that the measurement of the mean pressure and the mean velocity will permit the evaluation of the expression for the apparent eddy viscosity.

The mean velocity just prior to valve closure may be exactly determined from the Allievi<sup>1</sup> theory for the initial surge pressure due to sudden valve closure:

$$\left. \begin{aligned} P_o &= \rho \bar{u} a \\ \text{or} \\ \bar{u} &= \frac{P_o}{\rho a} \end{aligned} \right\} \quad (35)$$

Consider a pipeline as shown in Figure 14a in which a fluid is flowing with a mean velocity  $\bar{u}$  from the sending end to the receiving end. At point O is a valve which may be closed instantaneously. Figure 14b is a graphic representation of the pressure causing the mean flow in the pipeline, in which;

1.  $P_L$  is the pressure L feet from O or the pressure at the sending end prior to valve closure.
2.  $P_1$  is the pressure at the valve prior to closure.
3.  $\bar{p}$  is the differential pressure causing a mean velocity of  $\bar{u}$  in L feet of pipe.

When the valve is closed instantaneously, the pressure at O will rise to a value of  $P_2$ , a rise of  $P_o$  above  $P_1$ . The surge of pressure will be propagated in the direction of the sending end. At some point x



distance from 0, the rise above the hydraulic grade line is  $P_x$ .

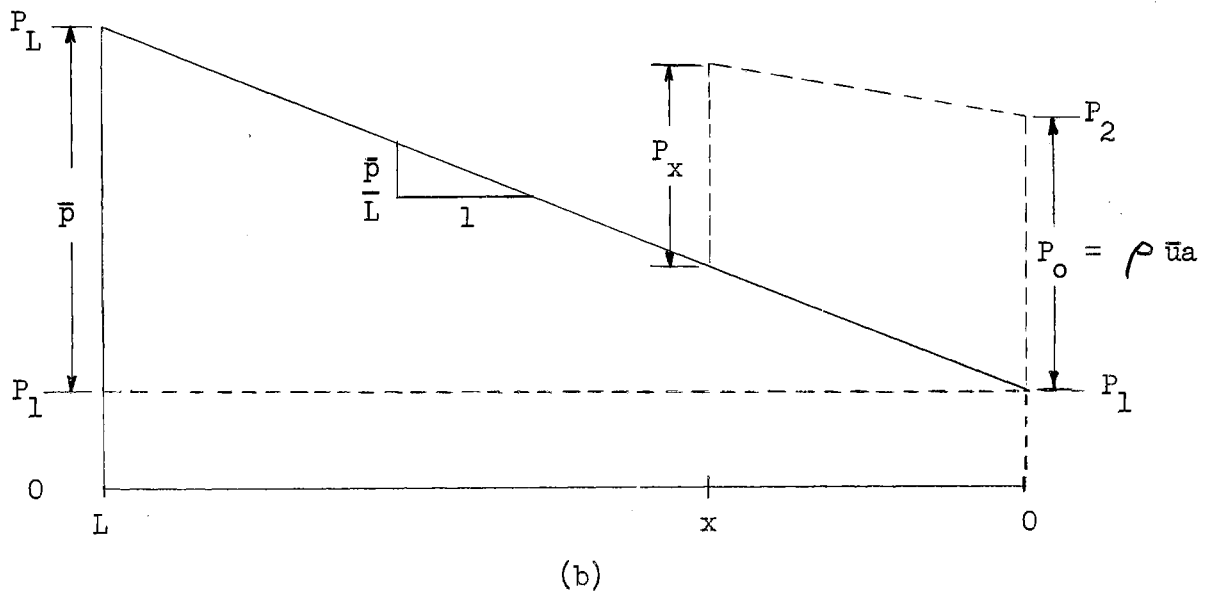
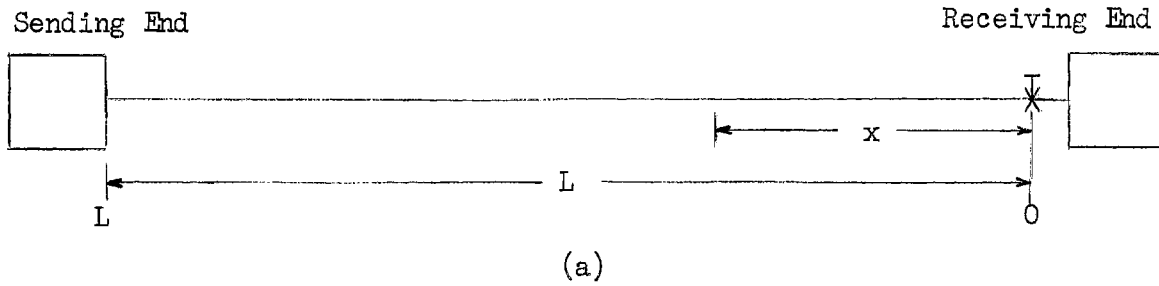


Figure No. 14

#### Definition Sketch for Water Hammer

Establishing a given flow in the pipeline system, closing the valve at 0 instantaneously and taking simultaneous traces (see Figure 15 for typical trace of pressure at the valve) at the points 0 and  $x$  (equal to twice the length in this case), the values of  $P_0$ ,  $P_x$  and "a" may be determined.  $P_0$  is the initial rise of pressure in psi.  $P_x$  is the rise above the hydraulic grade line at a distance  $X$  from 0 in psi. The velocity of propagation is determined by measuring the time  $\Delta t$  re-

quired for the surge to travel a known distance  $\Delta x$ ; then  $a = \frac{\Delta x}{\Delta t}$ . The mean velocity may then be calculated from Eq. 35. These data are recorded in Table I.

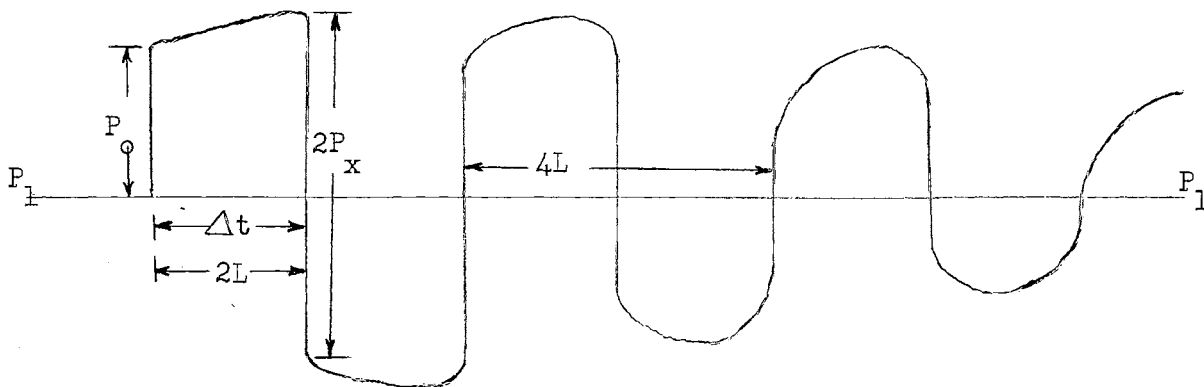


Figure 15

Typical Trace

Knowing the mean velocity, pipe diameter and the fluid properties, the Reynolds Number may be computed. The pipeline had been in use only a short time before the data reported herein were taken. A rust inhibitor had been added at the outset. Therefore, the pipe was assumed to be smooth. Values of the Darcy-Wiesbach resistance coefficient "f" were taken from Figure 108, page 203 of "Elementary Mechanics of Fluids" by Hunter Rouse. Eq. 33 was used to determine the values of the mean pressure. These data are recorded in Table II.

Making use of the data in Tables I and II, values of the apparent eddy viscosity may be computed from Eq. 34. The dimensionless para-

meter,

$$\Phi = \frac{\bar{\eta}}{\mu} \quad (36)$$

is plotted in Figure 16 versus the Reynolds Number.

The dotted line in Figure 16 represents the results of Murphree's<sup>10</sup> calculations as given below:

Murphree's Data

$N_R$	$\Phi$
3,000	7.2
5,000	11.7
10,000	20.0
25,000	42.0
50,000	72.0
100,000	121.0

At a Reynolds Number of 2,100 ( $\bar{u} = .165$  fps and  $\mu = 2.04 \times 10^{-5}$  lb.sec/ft<sup>2</sup>) and "f" equal .03,  $\bar{p}$  as determined from Eq. 33 is .107 psi.

Murphree's data gives a value of 5.65 for  $\Phi$ , or  $\bar{\eta} = 11.52 \times 10^{-5}$  lb.sec/ft<sup>2</sup>. Substituting this value into Eq. 34 a value of .142 psi is obtained for  $\bar{p}$ . The percentage difference from the actual value is:

$$\left( \frac{.142 - .107}{.107} \right) (100) = 32.7\%$$

A check of Figure 16 shows that Murphree's data will indicate too large a mean pressure drop below a Reynolds Number of about 13,000 and too small a value above this point.

Since Eq. 33 was used to get the  $\bar{p}$  used in Eq. 34 in calculating  $\bar{\eta}$ , substitution of any values from Figure 16 back into Eq. 34 will give the same result as Eq. 33.

TABLE I  
BASIC EXPERIMENTAL DATA

Run No.	P <sub>0</sub> psi	P <sub>x</sub> psi	a fps	$\bar{u}$ fps
1	104.5	86.2	4200	1.85
2	111.5	90.7	4200	1.97
3	116.2	94.2	4200	2.05
4	90.5	76.7	4200	1.60
5	107.0	88.5	4200	1.89
6	102.0	83.3	4200	1.80
7	109.0	88.2	4200	1.93
8	76.7	66.6	4200	1.36
9	104.5	86.0	4200	1.85
10	136.7	108.5	4380	2.31
11	141.2	110.7	4380	2.39
12	129.5	103.7	4380	2.19
13	150.8	117.8	4380	2.55
14	108.2	90.6	4380	1.83
15	129.5	103.7	4380	2.19
16	125.0	102.0	4380	2.12
17	104.5	85.5	4380	1.77
18	115.5	94.2	4380	1.95
19	89.6	76.5	4380	1.52
20	73.0	63.6	4380	1.23
21	94.2	80.2	4380	1.59
22	84.7	73.0	4380	1.43
23	84.7	73.0	4380	1.43
24	58.9	53.1	4380	.99
25	82.5	70.6	4380	1.39

TABLE I (cont.)

## BASIC EXPERIMENTAL DATA

Run No.	$P_o$ psi	$P_x$ psi	a fps	$\bar{u}$ fps
26	145.0	113.3	4380	2.45
27	134.1	108.1	4380	2.27
28	173.0	132.0	4380	2.93
29	166.5	125.8	4380	2.82
30	151.2	118.6	4380	2.56
31	166.5	129.7	4380	2.82
32	103.8	86.6	4380	1.76
33	121.1	99.5	4380	2.04
34	110.4	90.9	4380	1.87
35	170.2	130.2	4450	2.84
36	156.1	122.0	4450	2.60
37	150.2	119.7	4450	2.50
38	130.3	106.8	4450	2.17
39	105.7	89.2	4450	1.76
40	132.8	105.7	4450	2.21
41	124.5	100.3	4450	2.08
42	115.0	96.2	4450	1.92
43	94.0	80.8	4470	1.57
44	110.0	91.8	4470	1.83
45	92.6	78.6	4470	1.54
46	82.4	70.5	4470	1.37
47	83.8	72.0	4470	1.39
48	88.2	76.3	4470	1.46
49	67.6	59.6	4470	1.12
50	84.5	73.5	4470	1.41

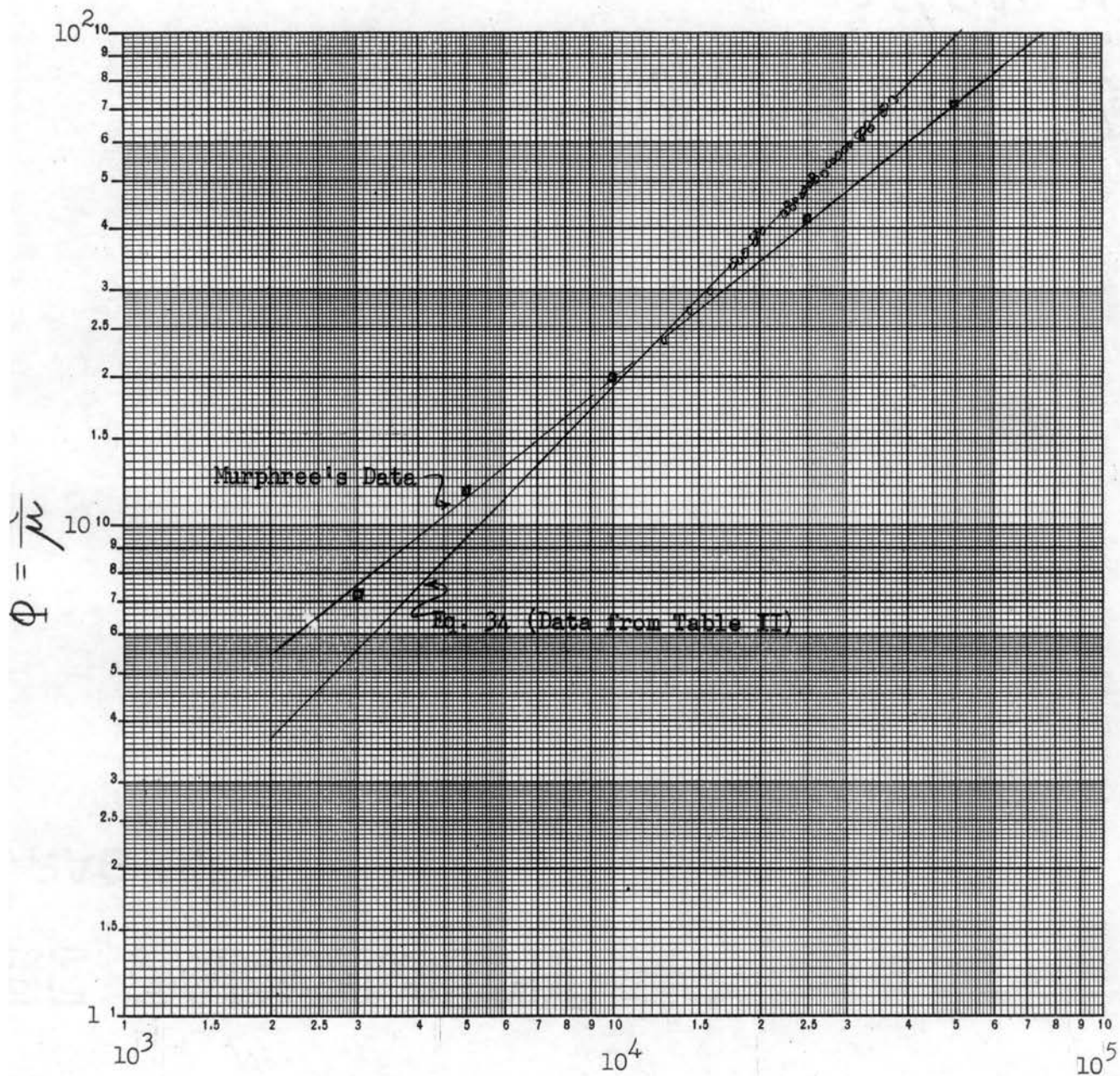
TABLE II  
 DETERMINATION OF THE  
 APPARENT EDDY VISCOSITY

Run No.	$N_R$ $\times 10^4$	$f$	$\bar{p}$ psi	$\bar{\eta}$ lb.sec/ft <sup>2</sup> $\times 10^{-5}$	$\bar{\Phi}$
1	2.36	.0255	10.32	93.26	45.70
2	2.51	.0250	11.64	99.66	48.80
3	2.61	.0248	12.50	103.06	50.60
4	2.04	.0265	7.86	80.16	39.30
5	2.41	.0254	10.75	94.96	46.50
6	2.29	.0256	9.83	90.86	44.50
7	2.46	.0253	11.18	97.06	47.60
8	1.74	.0276	5.79	67.56	33.10
9	2.36	.0255	10.32	93.26	45.70
10	2.95	.0242	15.70	116.96	57.30
11	3.05	.0240	16.70	120.46	59.10
12	2.79	.0245	14.20	110.96	54.30
13	3.25	.0236	18.80	128.46	63.00
14	2.33	.0255	10.10	92.06	45.20
15	2.79	.0245	14.20	110.96	54.30
16	2.70	.0253	13.40	105.96	51.80
17	2.26	.0258	9.50	88.96	43.50
18	2.49	.0252	11.40	98.26	48.15
19	1.94	.0268	7.12	75.76	37.10
20	1.57	.0282	4.78	61.06	29.90
21	2.03	.0265	7.76	79.56	39.00
22	1.82	.0272	6.35	71.16	34.85
23	1.82	.0272	6.35	71.16	34.85
24	1.26	.0295	3.18	48.96	23.95
25	1.77	.0272	6.01	69.16	33.85

TABLE II (Cont.)

DETERMINATION OF THE  
APPARENT EDDY VISCOSITY

Run No.	$N_R$ $\times 10^4$	f	$\bar{p}$ psi	$\bar{\eta}$ lb.sec/ft <sup>2</sup> $\times 10^{-5}$	$\Phi$
26	3.23	.0237	17.50	124.06	60.90
27	2.89	.0243	15.20	115.06	56.50
28	3.74	.0227	24.60	149.46	73.30
29	3.60	.0230	22.90	143.66	70.50
30	3.27	.0236	19.10	130.06	63.80
31	3.60	.0230	22.90	143.66	70.50
32	2.25	.0260	9.40	88.06	43.10
33	2.60	.0250	12.42	102.86	50.30
34	2.39	.0255	10.56	94.36	46.10
35	3.62	.0230	23.30	145.16	71.20
36	3.32	.0235	19.62	131.76	64.55
37	3.19	.0237	18.35	127.66	62.50
38	2.77	.0245	13.95	109.86	53.80
39	2.25	.0258	9.40	88.46	43.20
40	2.82	.0245	14.42	111.66	54.70
41	2.65	.0248	12.87	104.86	51.40
42	2.45	.0252	11.10	97.46	47.70
43	2.00	.0265	7.60	78.96	38.70
44	2.33	.0255	10.10	92.16	45.10
45	1.96	.0265	7.34	77.76	38.10
46	1.75	.0274	5.86	68.16	33.40
47	1.77	.0273	6.04	69.36	34.00
48	1.86	.0268	6.61	72.56	35.60
49	1.43	.0286	4.02	55.76	27.30
50	1.80	.0272	6.20	70.56	34.60



$$N_R = \frac{D\bar{u}\rho}{\mu}$$

Figure No. 16

$\Phi$  vs. Reynolds Number



CHAPTER VI  
 EXPERIMENTAL VERIFICATION OF THE VALUE  
 OF  
 THE APPARENT EDDY VISCOSITY

In the development of Eq. 30, the quantity  $\rho \overline{v'u'}$  was found to represent a rate of momentum transfer. Therein,  $u'$ , may be regarded as equal to  $\frac{\partial u}{\partial r} l$  where  $l$  is the distance between zones of flow or the Prandtl mixing length. Therefore,  $\rho \overline{v'u'}$  may be written  $\rho \overline{v'l} \frac{\partial u}{\partial r}$ . But  $\rho \overline{v'l}$  is mass times velocity times length or  $\rho E$  which is  $\eta$ . (see Eq. 4) or

$$\eta = -\rho \overline{v'l} \quad . \quad (18)$$

The fluid density,  $\rho$ , is the only known quantity in Eq. 18. Since the deviation from the mean velocity,  $v'$ , and the Prandtl mixing length,  $l$ , are incapable of measurement,  $\eta$  cannot be calculated directly.

All quantities in Eq. 30 are known or may be readily determined. Hence,  $\eta$  may be calculated. To verify this value some quantity involving the concept of  $\eta$ , which may also be evaluated by other means, is needed.

The attenuation coefficient,  $\alpha$ , for the damping of a pressure wave traveling in a liquid filled conduit presents a straight forward approach. For a damped oscillatory motion due to a unit pulse or water hammer,

$$P_x = P_0 e^{-\alpha x} \quad (37)$$

where  $P_0$  is the initial pressure rise,  $P_x$  is the pressure rise above the hydraulic grade line at some distance  $x$  and  $\alpha$  is the damping or

attenuation coefficient. For  $x = 2L$

$$\frac{P_x}{P_o} = \frac{1}{e^{2\alpha L}}$$

or

$$2\alpha L = \ln \frac{P_o}{P_x}$$

whence

$$\alpha = \frac{1}{2L} \ln \frac{P_o}{P_x} \quad (38)$$

The experimental values of  $\alpha$  in Table III are obtained from the values of  $P_o$  and  $P_x$  in Table I. These data are plotted in Figure 17. The line was fitted by the method of least squares.

The theoretical expression for the attenuation coefficient, proposed and verified by Waller, Fristoe et al<sup>17</sup>, is

$$\alpha_w = \frac{n\bar{p}A}{2L\bar{q}\rho_a} \quad (39)$$

But from Eq. 30

$$\frac{\bar{p}}{L} = \frac{(\mu + \bar{\eta})(8)(1.43 \sqrt{f})\bar{u}}{R^2} \quad (40)$$

whence  $\alpha$  in terms of the apparent eddy viscosity is

$$\alpha_K = \frac{4n(\mu + \bar{\eta})(1.43 \sqrt{f})}{\rho_a R^2} \quad (41)$$

The values of  $\alpha_K$  in Table IV were calculated from the data in Table II. The value,  $\alpha_{L.S.}$ , is the least squares value of  $\alpha_{exp.}$

for a given  $\bar{\Phi}$  value. The percentage difference shown in Table IV was based on the least squares value of  $\alpha_{\text{exp}}$ .

It should be noted that all values of  $\alpha_K$  were less than  $\alpha_{\text{L.S.}}$ . This is to be expected since all higher order differentials were neglected in the Prandtl mixing length theory. A further examination of all the data and the conditions under which it was taken reveals that neglecting differentials of higher order is of little consequence. Runs one through nine were made in early March when the building was closed to the outdoors and heated to approximately 70° Fahrenheit. The remaining runs were taken in late March, April and May after fans had been installed in the basement, it was not closed to the outdoors and the temperature was somewhat above 70° F.

The bulk modulus of water increases with rising temperature. An increase in the bulk modulus gives an increase in the velocity of propagation. Inspection of Eq. 41 reveals that this would reduce the value of  $\alpha_K$ .

Further, an increase in the velocity of propagation results in an increase in the mean velocity and the mean pressure. The dynamic viscosity decreases with rising temperature. The net result being an increase in the apparent eddy viscosity and the Reynolds number. (see Eq. 33 and 34). Had the temperature been noted and the proper corrections made, the result would most likely have been comparable to that of the first nine runs.

As noted in Chapter V, the maximum probable error in measuring  $P_0$  was  $\pm 3.15$  psi. A change of  $\pm 3.15$  psi in  $P_0$  would result in a variation in  $\bar{\eta}$  of approximately  $\pm 3.50$  percent and a corresponding change in  $\alpha_K$  of about  $\pm 3.00$  percent.

Referring again to runs one through nine, even if all the discrepancies are charged against the theory, it can only be concluded that the results are within the precision of the instrumentation and Eq. 41

$$\alpha_K = \frac{4n(\mu + \bar{\eta})(1.43 \sqrt{F})}{\rho aR^2}$$

is correct and therefore, Eq. 30

$$\bar{\eta} = \frac{\bar{\rho}R^2}{8L(1.43 \sqrt{F})\bar{u}} - \mu$$

for the apparent eddy viscosity is valid.

TABLE III  
 EXPERIMENTAL DETERMINATION  
 OF THE ATTENUATION COEFFICIENT

Run No.	$\frac{P_o}{P_x}$	$\ln\left(\frac{P_o}{P_x}\right)$	$\alpha \text{ exp.}$ $\text{ft}^{-1} \times 10^{-5}$
1	1.215	.1949	4.68
2	1.230	.2070	4.97
3	1.235	.2110	5.07
4	1.180	.1658	3.98
5	1.210	.1910	4.59
6	1.225	.2030	4.88
7	1.237	.2125	5.11
8	1.152	.1415	3.40
9	1.215	.1949	4.68
10	1.260	.2310	5.54
11	1.275	.2430	5.83
12	1.250	.2235	5.37
13	1.280	.2470	5.93
14	1.195	.1782	4.29
15	1.250	.2235	5.37
16	1.225	.2030	4.89
17	1.223	.2010	4.84
18	1.225	.2030	4.88
19	1.172	.1590	3.83
20	1.148	.1383	3.32
21	1.175	.1615	3.89
22	1.160	.1486	3.57
23	1.160	.1486	3.57
24	1.110	.1045	2.51
25	1.168	.1555	3.74

TABLE III (Cont.)

EXPERIMENTAL DETERMINATION  
OF THE ATTENUATION COEFFICIENT

Run No.	$\frac{P_o}{P_x}$	$\ln\left(\frac{P_o}{P_x}\right)$	$\alpha_{exp.}$ $ft^{-1} \times 10^{-5}$
26	1.280	.2470	5.94
27	1.240	.2155	5.18
28	1.310	.2710	6.50
29	1.324	.2810	6.76
30	1.275	.2430	5.85
31	1.285	.2510	6.03
32	1.200	.1825	4.39
33	1.217	.1967	4.72
34	1.215	.1955	4.70
35	1.308	.2685	6.46
36	1.280	.2470	5.94
37	1.255	.2275	5.47
38	1.220	.1995	4.80
39	1.184	.1690	4.06
40	1.255	.2280	5.48
41	1.240	.2150	5.17
42	1.195	.1785	4.29
43	1.163	.1512	3.63
44	1.200	.1825	4.39
45	1.179	.1650	3.97
46	1.168	.1555	3.74
47	1.164	.1520	3.65
48	1.156	.1450	3.49
49	1.135	.1265	3.04
50	1.150	.1400	3.36

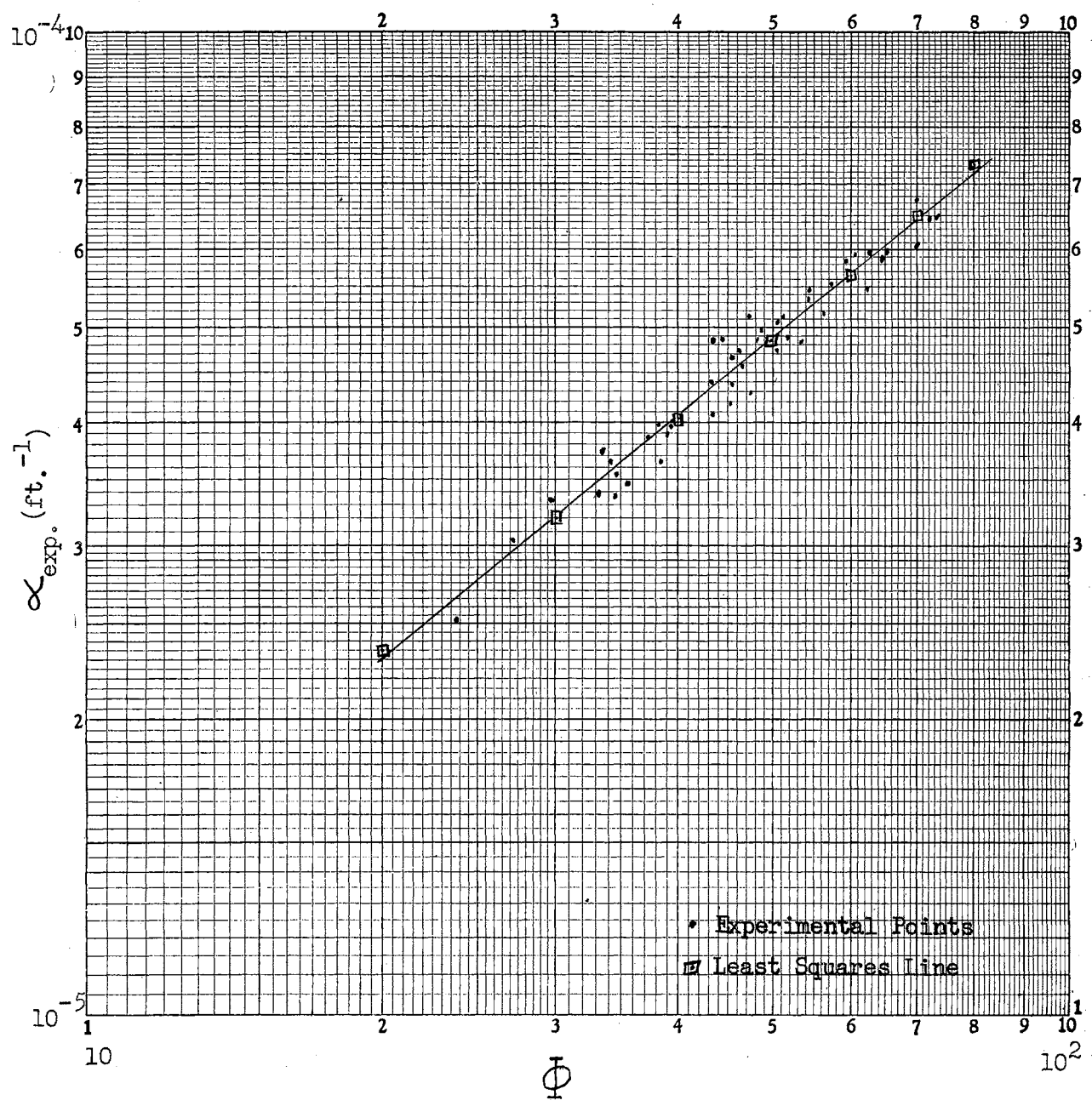


Figure No. 17

$\alpha_{\text{exp.}}$  vs.  $\Phi$

TABLE IV  
 DETERMINATION OF THE ATTENUATION  
 COEFFICIENT IN TERMS OF THE APPARENT EDDY VISCOSITY

Run No.	$\alpha_K$ ft <sup>-1</sup> x 10 <sup>-5</sup>	$\alpha_{L.S.}$ ft <sup>-1</sup> x 10 <sup>-5</sup>	% Difference $(\frac{\alpha_K - \alpha_{L.S.}}{\alpha_{L.S.}})100$
1	4.48	4.50	- .45
2	4.74	4.75	- .20
3	4.89	4.90	- .20
4	3.94	4.00	-1.50
5	4.55	4.59	- .87
6	4.37	4.42	-1.13
7	4.65	4.65	- .00
8	3.41	3.47	-1.73
9	4.49	4.51	- .44
10	5.23	5.43	-3.68
11	5.37	5.59	-3.93
12	5.00	5.20	-3.85
13	5.66	5.90	-4.07
14	4.25	4.49	-5.34
15	5.00	5.20	-3.85
16	4.84	5.00	-3.20
17	4.13	4.35	-5.06
18	4.50	4.73	-4.86
19	3.60	3.81	-5.52
20	3.00	3.18	-5.66
21	3.75	3.97	-5.54
22	3.41	3.61	-5.54
23	3.41	3.61	-5.54
24	2.48	2.65	-6.41
25	3.32	3.52	-5.68



TABLE IV (Cont.)

DETERMINATION OF THE ATTENUATION  
COEFFICIENT IN TERMS OF THE APPARENT EDDY VISCOSITY

Run No.	$\alpha_K$ ft <sup>-1</sup> x 10 <sup>-5</sup>	$\alpha_{L.S.}$ ft <sup>-1</sup> x 10 <sup>-5</sup>	% Difference $\left(\frac{\alpha_K - \alpha_{L.S.}}{\alpha_{L.S.}}\right)100$
26	5.40	5.73	-5.76
27	5.16	5.38	-4.09
28	6.45	6.70	-3.73
29	6.25	6.47	-3.40
30	5.74	5.97	-3.85
31	6.25	6.47	-3.40
32	4.11	4.30	-4.42
33	4.68	4.89	-4.30
34	4.35	4.55	-4.39
35	6.20	6.52	-4.91
36	5.71	6.00	-4.84
37	5.55	5.85	-5.13
38	4.86	5.15	-5.64
39	4.04	4.32	-6.50
40	4.95	5.24	-5.54
41	4.67	4.99	-6.40
42	4.39	4.67	-6.00
43	3.66	3.95	-7.34
44	4.17	4.48	-6.92
45	3.60	3.90	-7.69
46	3.22	3.50	-8.00
47	3.27	3.54	-7.63
48	3.38	3.66	-7.65
49	2.71	2.95	-8.14
50	3.32	3.59	-7.52

## CHAPTER VII

### APPLICATIONS OF THE APPARENT EDDY VISCOSITY

As noted in Chapter VI, there are two quantities in the defining equation for  $\bar{\eta}$  that are incapable of measurement. Therefore, in using another quantity, involving the concept of  $\bar{\eta}$ , which may also be evaluated by other means, a direct application of  $\bar{\eta}$  is indicated.

#### A. ATTENUATION COEFFICIENT

The attenuation coefficient may be determined from experimental measurements and Eq. 38,

$$\alpha = \frac{1}{2L} \ln \frac{P_o}{P_x} \quad (38)$$

The Waller theory gives

$$\alpha_w = \frac{n\bar{\eta}A}{2L\bar{q}\rho a} \quad (39)$$

Eq. 41, involving the concept of  $\bar{\eta}$ , indicates

$$\alpha_K = \frac{4n(\mu + \bar{\eta})(1.43 \sqrt{f})}{\rho_{aR}^2} \quad (41)$$

Waller, Fristoe et al<sup>18</sup> demonstrated that Eq. 39 successfully predicted the actual happenings as indicated by Eq. 38. In Chapter VI it was shown that Eq. 41 gave values of  $\alpha$  comparable to Eq. 38 within the limits of the instrumentation.

Therefore, Eq. 41 may be regarded as a valid direct application of the concept of the apparent eddy viscosity to the attenuation of a

pressure wave traveling in a liquid filled conduit. In addition, Eq. 41 further verifies the Waller theory as expressed in Eq. 39.

#### B. HEAT TRANSFER COEFFICIENT

In 1874, Osbourne Reynolds<sup>16</sup>, in his treatise "On the Extent and Action of the Heating Surface for Steam Boilers" suggested that momentum and heat in a fluid are transferred in the same way. He concluded that in geometrically similar systems a simple proportionality relation must exist between fluid friction and heat transfer. Since that time, particularly in recent years, many authors have proposed existence of an apparent thermal conductivity due to the eddy motion in fluid flow.

The relationship in common use today for the heating of fluids in turbulent flow through circular conduits is the Dittus-Boelter<sup>6,9</sup> equation,

$$\frac{hD}{k} = 0.023 \left( \frac{\bar{u}D\rho}{\mu} \right)^{.8} \left( \frac{\mu}{\mu_c} \right)^{.4} \quad (42)$$

where  $h$  is the film coefficient of heat transfer,  $k$  is the thermal conductivity of the fluid,  $c_p$  is the specific heat at constant pressure and all other terms are as previously defined. It should be noted that the expression is in dimensionless form.

$$\text{Nusselt number} = N_N = \frac{hD}{k} \quad (43)$$

$$\text{Reynolds number} = N_R = \frac{\bar{u}D\rho}{\mu} \quad (44)$$

$$\text{Prandtl number} = N_P = \frac{\mu c_p}{k} \quad (45)$$

Eq. 42 was derived by the methods of dimensional analysis. The constant and the exponents represent the results of correlating a large

amount of experimental data.

Assuming

$$h = f(\bar{\eta}, \mu, k, D, c_p) \quad (46)$$

and proceeding with a dimensional analysis:

Variable	Symbol	Heat H	Time T	Length L	Mass M	Temp. $\theta$
Heat Trans- fer Coeff.	h	1	- 1	- 2	0	- 1
Eddy Viscosity	$\bar{\eta}$	0	- 1	- 1	1	0
Dynamic Viscosity	$\mu$	0	- 1	- 1	1	0
Thermal Conductivity	k	1	- 1	- 1	0	- 1
Diameter	D	0	0	1	0	0
Specific Heat	$c_p$	1	0	0	- 1	- 1
Constant	C	0	0	0	0	0

Eq. 46 may then be written

$$h = CD^a k^b c_p^c \mu^d \bar{\eta}^e \quad (47)$$

or the dimensional equation becomes

$$HT^{-1}L^{-2}\theta^{-1} = (L^a)(HT^{-1}L^{-1}\theta^{-1})^b(HM^{-1}\theta^{-1})^c(T^{-1}L^{-1}M)^d(T^{-1}L^{-1}M)^e \quad (48)$$

If Eq. 48 is to be dimensionless, exponents of dimensions of the left member must equal exponents of the dimensions of the right member.

Thus

$$\begin{aligned}
 \text{H:} \quad & 1 = b + c \\
 \text{T:} \quad & -1 = -b - d - e \\
 \text{L:} \quad & -2 = a - b - d - e \\
 \text{\(\theta\):} \quad & -1 = -b - c \\
 \text{M:} \quad & 0 = -c + d + e
 \end{aligned}$$

Solving these equations simultaneously it is found that

$$\begin{aligned}
 a &= -1 \\
 b &= 1 - c \\
 d &= c - e
 \end{aligned}$$

and Eq. 47 becomes

$$\frac{hD}{k} = C \left( \frac{\mu^c}{k} \right)^c \left( \frac{\bar{\eta}}{\mu} \right)^e \quad (49)$$

This equation is identical to the Dittus-Boelter equation except that  $\frac{\bar{\eta}}{\mu} = \phi$  replaces the Reynolds number. An expression directly connecting fluid friction ( $\bar{\eta}$ ) and heat transfer (h) is thus obtained.

Assuming that the Nusselt number varies as the four-tenths power of the Prandtl number Eq. 49 becomes,

$$\frac{hD}{k} = C \left( \frac{\mu^c}{k} \right)^{.4} \left( \frac{\bar{\eta}}{\mu} \right)^e \quad (50)$$

For a mean temperature of 70° F,  $\mu = 2.36$  lb./hr.ft.,  
 $c_p = 1$  B/lb.° F,  $k = .343$  B/hr.ft.° F and  $D = .134$  ft.,  
 Eq. 42 becomes

$$h_{in} = .1275 (N_R)^{.8} \quad (51)$$

For the various Reynolds numbers shown, the following heat transfer coefficients are obtained:

$N_R$	$h_{in}$ B/hr.ft. <sup>2</sup> ° F	$\Phi$
10,000	202	18.6
20,000	352	38.3
30,000	486	58.7
40,000	613	80.0
50,000	732	101.0

The values of the heat transfer coefficient are plotted versus  $\Phi$  in Figure 19. The values of  $\Phi$  corresponding to the given Reynolds number as obtained from runs one through nine are plotted in Figure 18.

From the plot in Figure 19,

$$h_{in} = 21.6 \Phi^{.765}$$

at a Prandtl number of 6.88,  $T = 70^\circ \text{ F}$ ,  $D = .134 \text{ ft.}$  and  $k = .343 \text{ B/hr. ft.}^\circ \text{ F}$ .

Whence

$$\frac{hD}{k} = 21.6 \Phi^{.765} \left( \frac{.134}{.343} \right) = 8.45 \Phi^{.765}$$

Substituting these values in Eq. 50

$$\frac{hD}{k} = C \left( \frac{\mu^c}{k} \right)^{.4} \left( \frac{\bar{\eta}}{\mu} \right)^e = 8.45 \Phi^{.765}$$

$$C(6.88)^{.4} = 8.45$$

$$C = 3.91$$

Whence

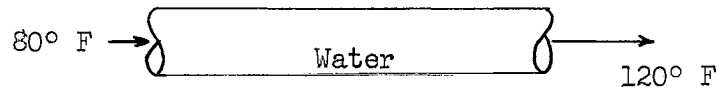
$$\frac{hD}{k} = 3.91 \left( \frac{\mu^c}{k} \right)^{.4} \left( \frac{\bar{\eta}}{\mu} \right)^{.765}$$

or

$$N_N = 3.91 (N_P)^{.4} (\Phi)^{.765} \quad (52)$$

To demonstrate the validity of this expression two examples are shown comparing the results of the Dittus-Boelter equation, Eq. 42, and Eq. 52 involving  $\bar{\Phi}$ .

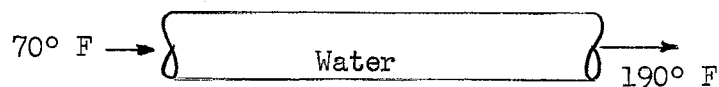
Example 1<sup>6a</sup>



$$\begin{aligned}
 T_{\text{mean}} &= 100^{\circ} \text{ F} \\
 \text{I.D.} &= .25 \text{ inches} \\
 \mathcal{V} &= .0268 \text{ ft.}^2/\text{hr.} \\
 \bar{u} &= 4750 \text{ ft./hr.} \\
 N_R &= 3685 \\
 k &= .359 \text{ B/hr.ft.}^{\circ} \text{ F} \\
 c_p &= 1 \text{ B/lb.}^{\circ} \text{ F} \\
 N_p &= 4.63 \\
 h &= 512 \text{ B/hr.ft.}^2 \text{ }^{\circ} \text{ F} \text{ (Dittus-Boelter Eq.)} \\
 \bar{\Phi} &= 6.4 \text{ (Figure 18)}
 \end{aligned}$$

From Eq. 52

$$\begin{aligned}
 h &= \frac{(.359)(3.91)(4.63)^{.4}(6.4)^{.765}}{\frac{.25}{12}} \\
 h &= (67.25)(1.847)(4.14) \\
 h &= 514 \text{ B/hr.ft.}^2 \text{ }^{\circ} \text{ F} \\
 \% \text{ Diff} &= \left( \frac{514 - 512}{512} \right) (100) = +.39\%
 \end{aligned}$$

Example 2<sup>6b</sup>

$$T_{\text{mean}} = 130^{\circ} \text{ F}$$

$$\nu = .0201 \text{ ft.}^2/\text{hr.}$$

$$\text{I.D.} = 4 \text{ inches}$$

$$\bar{u} = 4640 \text{ ft./hr.}$$

$$N_R = 77,000$$

$$k = .372 \text{ B/hr.ft.}^{\circ} \text{ F}$$

$$c_p = 1 \text{ B/lb.}^{\circ} \text{ F}$$

$$N_p = 3.33$$

$$h = 337 \text{ B/hr.ft.}^2 \text{ }^{\circ} \text{ F (Dittus-Boelter Eq.)}$$

$$\Phi = 158 \text{ (Figure 18)}$$

From Eq. 52

$$h = \frac{(.372)(3.91)(3.33)^{.4}(158)^{.765}}{\frac{4}{12}}$$

$$h = (4.36)(1.618)(48.3)$$

$$h = 341 \text{ B/hr.ft.}^2 \text{ }^{\circ} \text{ F}$$

$$\% \text{ Diff} = \left( \frac{341 - 337}{337} \right) (100) = + 1.19 \% .$$

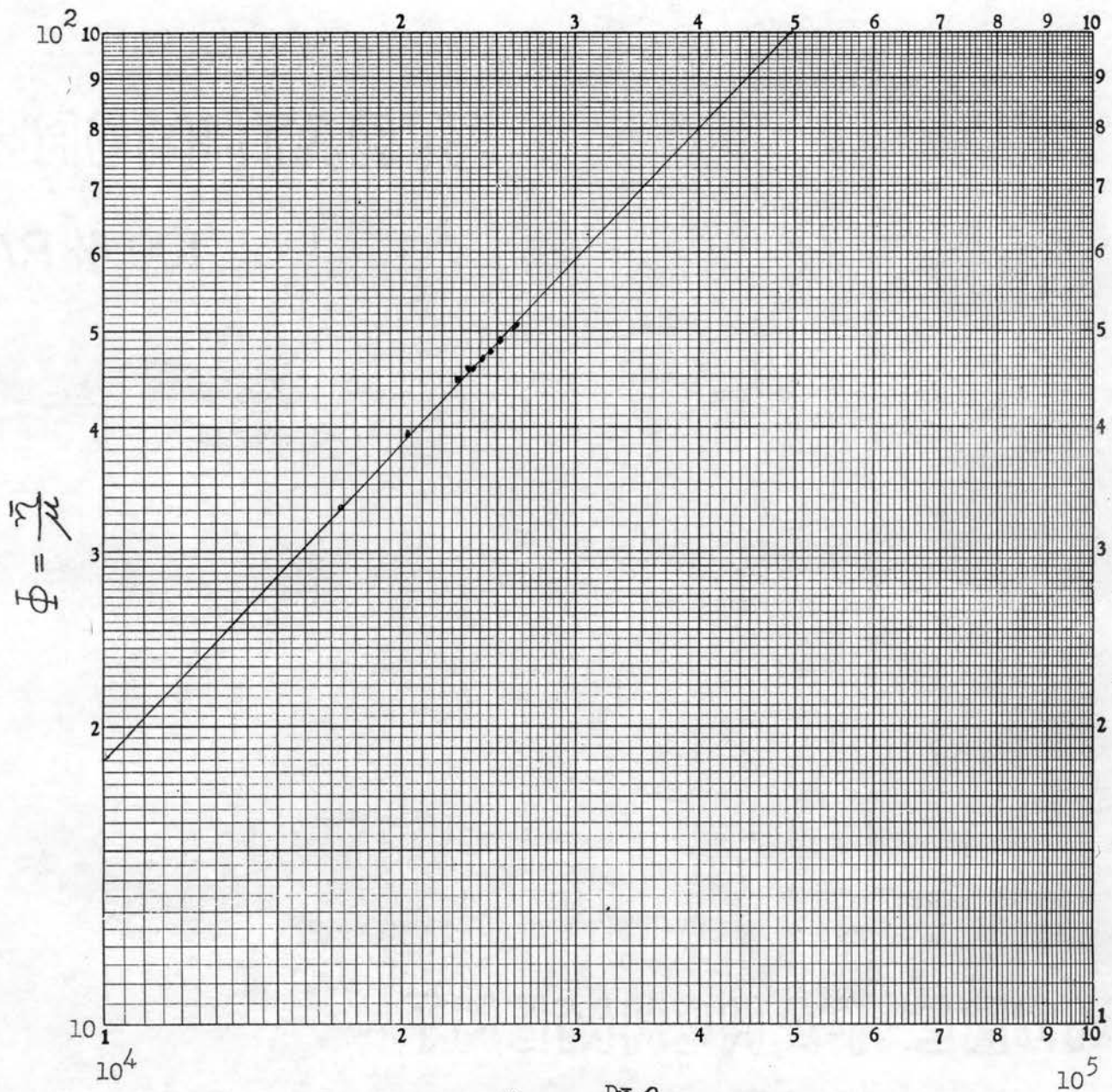
The data reported in this thesis were taken at a temperature of approximately 70° F on a 1.61 inch inside diameter pipe using water, over a Reynolds number range of 12,600 - 37,400. In Example 1, the fluid is water,  $T_{\text{mean}}$  equals 100° F, I.D. = .25 inches and  $N_R = 3685$ . In Example 2, the fluid is water,  $T_{\text{mean}} = 130^{\circ} \text{ F}$ , I.D. = 4 inches and  $N_R = 77,000$ .



Thus, from this brief analysis, it appears that:

1. The heat transfer coefficient for the heating of water in turbulent flow in a circular conduit may be directly expressed as a function of the apparent eddy viscosity, and

2. The apparent eddy viscosity is essentially independent of temperature and dependent only on the flow regime.



$$N_R = \frac{D U \rho}{\mu}$$

Figure No. 18

$\Phi$  vs. Reynolds Number

(Runs 1 - 9)

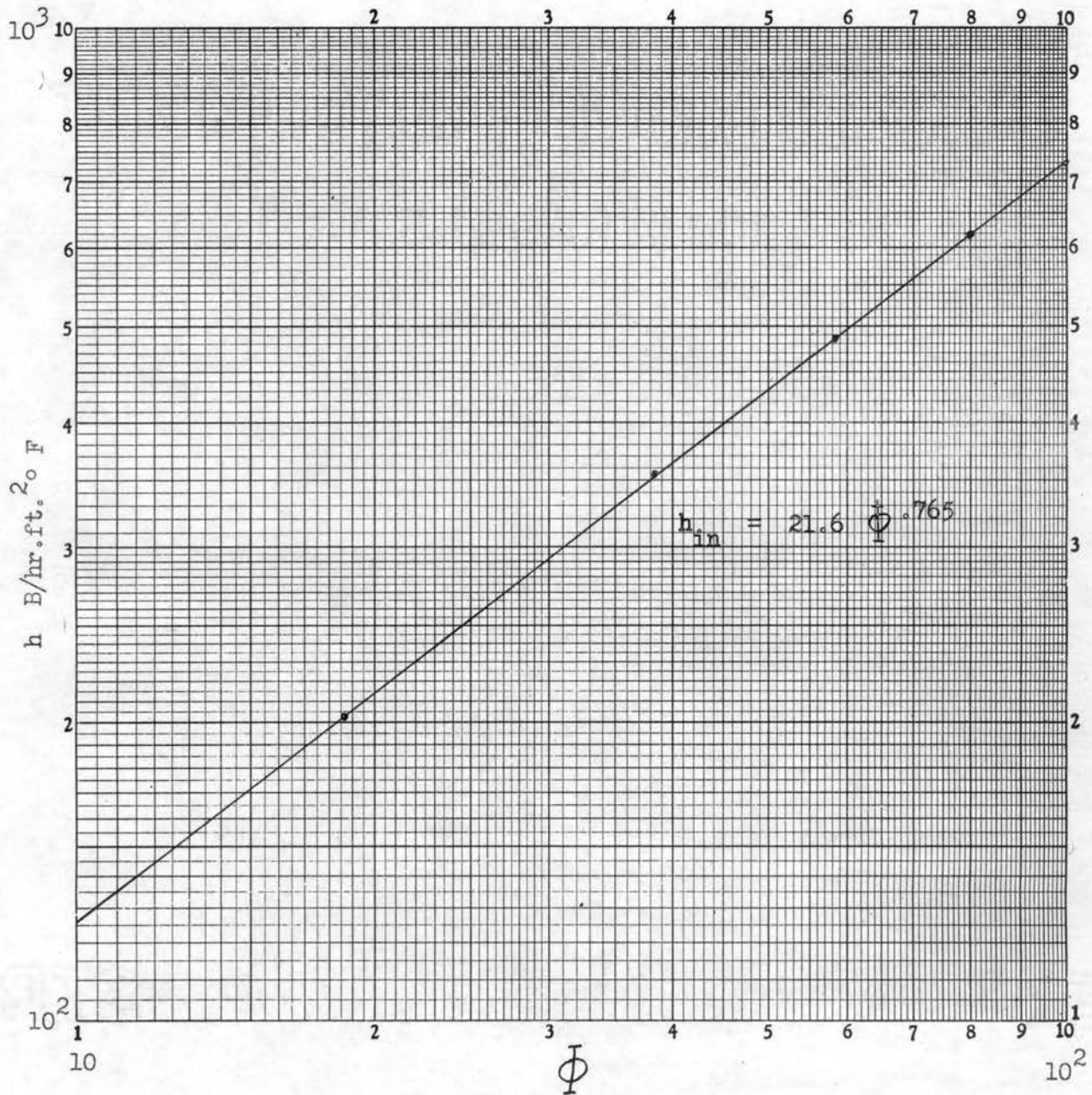


Figure No. 19

Heat Transfer Coefficient vs.  $\Phi$ 
 $D = .134 \text{ ft.}; T = 70^\circ \text{ F}; N_p = 6.88$

## CHAPTER VIII

### SUMMARY AND CONCLUSIONS

Many attempts have been made to relate fluid friction, momentum transfer and heat transfer. All too frequently the results have been in such complex form that they are not any great assistance to the practicing engineer.

The expression (Eq. 30) for the apparent dynamic eddy viscosity developed herein is directly solvable and involves only the dimensions of the conduit and well known fluid properties. This expression is a direct relationship between momentum transfer and fluid friction.

From the results of the mathematical derivation presented in Chapter IV and the experimental work presented in Chapter V it can only be concluded that:

1. The principle of superposition holds for this case and the total velocity at a point is equal to the sum of the mean velocity at that point and the deviation from the mean velocity at that point;

2. The Prandtl mixing length theory, although not mathematically rigorous, is valid. While it is difficult to conceive of a mass of fluid, however small, traveling a given distance and then suddenly losing a part of its momentum to the surrounding flow in a continuous, homogeneous and isotropic fluid, the Prandtl theory does satisfactorily account for the secondary motion and is therefore valid.

3. The Navier-Stokes equations are equally applicable to turbulent as well as laminar flow since the temporal mean value of the apparent dynamic eddy viscosity accounts for the additional dissipative forces at work in the fluid;

4. The effects of neglecting higher order differentials is negligible.

In addition, the shearing stress at any point in a fluid in turbulent motion may be determined directly from Eq. 2 for a given velocity distribution since a sufficiently exact value of the apparent dynamic eddy viscosity is now available. To date, this has not been possible as no data were available on the contribution of the eddy motion to the dissipative action in the fluid.

The results of applying the concept of the apparent dynamic eddy viscosity to the attenuation of a pressure wave in a liquid filled conduit (see Eq. 41) not only further verifies the Waller theory in this regard but gives another method of determining the attenuation coefficient.

The analysis presented in Chapter VI shows the applicability of momentum transfer to heat transfer work. From the limited amount of data available it appears that the resulting expression for the transfer of heat from the pipe wall to the fluid flowing therein is valid and that the apparent dynamic eddy viscosity is essentially independent of temperature.

The mathematical procedure used is perfectly general and could be applied to flow through annuli and flow past flat plates providing velocity distributions are known for these flow regimes. It now remains for further experimental work to be done to obtain values of the apparent dynamic eddy viscosity over a wider range of Reynolds numbers, with different fluids and at various temperatures to substantiate the results reported herein.

## BIBLIOGRAPHY

1. Allievi, Lorenzo. General Theory of Perturbed Flow of Water in Conduits. Milan, 1903. Translated by E. E. Halmos, 1925.
2. Bahkmeteff, Boris A. The Mechanics of Turbulent Flow. Princeton: Princeton University Press, 1941. pp. 39-41.
3. Binder, R. C. Advanced Fluid Dynamics and Fluid Machinery. New York: Prentice-Hall, Inc., 1951. p. 98.
4. Binder, R. C. "The Damping of Large Amplitude Vibrations of a Fluid in a Pipe" Journal of Acoustical Society of America, Vol. 15, No. 1, July, 1943. pp. 41-43.
5. Dryden, Hugh L. "The Turbulence Problem Today" The Proceedings of the First Midwestern Conference on Fluid Dynamics, Champaign: University of Illinois, 1950. pp. 1-4.
  - 5a. Ibid. pp. 6-7.
  - 5b. Ibid. p. 2.
6. Jakob, Max, and G. A. Hawkins. Elements of Heat Transfer and Insulation. New York: John Wiley & Sons, Inc., 1950. p. 113.
  - 6a. Ibid. p. 117.
  - 6b. Ibid. p. 117.
7. Kaplan, Wilfred. Advanced calculus. Cambridge: Addison-Wesley Publishing Company, 1952. pp. 616-617.
8. Lamb, Sir Horace. Hydrodynamics. New York: Dover Publications, 1945. p. 577.
9. McAdams, W. H. Heat Transmission. New York: McGraw-Hill Book Company, Inc., 1942. p. 168.
10. Murphree, E. V. "Relation Between Heat Transfer and Fluid Friction" Industrial and Engineering Chemistry. Vol. 24, 1932. p. 726.
11. Phillips, H. B. Vector Analysis. New York: John Wiley & Sons, Inc., 1953. pp. 103-104.
12. Prandtl, Ludwig. Fluid Dynamics. New York: Hafner Publishing Company, 1952. p. 85.
  - 12a. Ibid. p. 117.

- 12b. Ibid. p. 117.
- 12c. Ibid. p. 85.
- 12d. Ibid. pp. 85-86.
- 12e. Ibid. pp. 117-118.
13. Rohsenow, Warren M. "Analogy Between Heat Transfer and Momentum Transfer" Unpublished Proceedings of Heat Transfer Short Course. Oklahoma A & M College, April, 1955. pp. 21-43.
14. Rouse, Hunter. Elementary Mechanics of Fluids. New York: John Wiley & Sons, Inc., 1946. p. 179.
- 14a. Ibid. p. 179.
- 14b. Ibid. pp. 193-198.
- 14c. Ibid. p. 157.
- 14d. Ibid. p. 158.
15. Rouse, Hunter. Fluid Mechanics for Hydraulic Engineers. New York: McGraw-Hill Book Company, Inc., 1938. pp. 176-178.
- 15a. Ibid. p. 185.
16. von Karman, Theodore. "The Analogy Between Fluid Friction and Heat Transfer" Transactions of the American Society of Mechanical Engineers. Vol. 61., 1939. p. 705.
17. Waller, E. J. "Fundamental Analysis of Unsteady Pressure Variations in Pipeline Systems", Stillwater: Oklahoma A & M College Engineering Experiment Station Publication No. 92, 1954. p. 37 rev.
18. Waller, E. J., H. T. Fristoe and J. R. Norton. "Report on Unit Pulse Tests at Oklahoma A & M College" Unpublished Report to Project Donors, 1955. p. 63.

VITA

Robert Donavon Kersten  
candidate for the degree of  
Master of Science

Thesis: DEVELOPMENT OF AN ANALYTICAL EXPRESSION FOR THE APPARENT  
EDDY VISCOSITY OF A FLUID IN TURBULENT MOTION IN A CIRCULAR  
PIPE.

Major: Civil Engineering (Fluid Mechanics).

Biographical and Other Items:

Born: January 30, 1927 at Carlinville, Illinois.

Undergraduate Study: Westminster College, 1945; Yale University, 1945-1946; Northwestern University, 1946; O.A.M.C., 1947-1949.

Graduate Study: O.A.M.C., 1954-1956.

Experiences: U. S. Naval Air Corps, 1945-1947; Laboratory Assistant, 1947; Hydraulic Engineer, U. S. Department of the Interior, 1949-1953; Research Associate, Oklahoma A & M College, 1953-1956.

Publication: "Reciprocating Pump Tests on a Pilot Pipeline System" by E. J. Waller and R. D. Kersten. Pressure Surge Research Project Report No. 2., Nov. 1955.

Member of Pi Gamma Mu, Sigma Tau, Chi Epsilon, and Junior Member of the American Society of Civil Engineers.

Date of Final Examination: January, 1956.



THESIS TITLE: DEVELOPMENT OF AN ANALYTICAL EXPRESSION FOR THE  
APPARENT EDDY VISCOSITY OF A FLUID IN TURBULENT  
MOTION IN A CIRCULAR PIPE.

AUTHOR: Robert Donavon Kersten

THESIS ADVISER: Prof. Roger L. Flanders

The content and form have been checked and approved by the author and thesis adviser. The Graduate School Office assumes no responsibility for errors either in form or content. The copies are sent to the bindery just as they are approved by the author and faculty adviser.

TYPIST: Fern B. Hall